Instituto Tecnológico y de Estudios Superiores de Monterrey

Campus Monterrey

School of Engineering and Science


# Design of a model for multi axis measuring machines to analyze error positioning in Gantry systems

A thesis presented by

José Gustavo Anaya Aranda

Submitted to the
School of Engineering and Sciences
In partial fulfillment of the requirements for the degree of

Master of Science

In

Manufacturing Systems

Monterrey Nuevo León, December 10, 2019

Instituto Tecnológico y de Estudios Superiores de Monterrey

Campus Monterrey

School of Engineering and Sciences

The committee members, hereby, certify that have read the thesis presented by José Gustavo Anaya Aranda and that is fully adequate in scope and quality as a partial requirement for the degree of Master of Science in Manufacturing Systems,

_____
Dr. Horacio Ahuett Garza
Tecnológico de Monterrey
School of Engineering and Sciences
Principal Advisor

_____
MEng. Pedro Antonio Orta Castañon
Tecnológico de Monterrey
Committee Member

_____
Dr. Pedro Daniel Urbina Coronado
Tecnológico de Monterrey
Committee Member

_____
Dr. Rubén Morales Menéndez
Dean of Graduate Studies
School of Engineering and Sciences

Monterrey Nuevo León, December 10, 2019

## Declaration of Authorship

I, José Gustavo Anaya Aranda, declare that this dissertation titled, “Design of a model for multi axis measuring machines to analyze error positioning in Gantry systems” and the work presented in it are my own. I confirm that:

- This work was done wholly or mainly while in candidature for a research degree at this University.
- Where any part of this dissertation has previously been submitted for a degree or any other qualification at this University or any other institution, this has been clearly stated.
- Where I have consulted the published work of others, this is always clearly attributed.
- Where I have quoted from the work of others, the source is always given. With the exception of such quotations, this dissertation is entirely my own work.
- I have acknowledged all main sources of help.
- Where the dissertation is based on work done by myself jointly with others, I have made clear exactly what was done by others and what I have contributed myself.

_____

José Gustavo Anaya Aranda
Monterrey Nuevo León, December 10th, 2019

## Dedication

To my dear and loving parents and brothers, with their unconditional confidence, support, patience, and encouragement.

## Acknowledgments

I would like to express my deepest gratitude to all those who have been side by side with me.
To God for his care and protection.
To my advisors for guiding me during this period.
To Tecnológico de Monterrey that supported me with tuition.
To CONACYT with the support for living.

Design of a model for multi axis measuring machines to analyze error positioning in Gantry systems
by

José Gustavo Anaya Aranda

**Abstract**

There have been cases in which poor quality control has threaten a company's survival. This has caused that clients keeps demanding for higher quality products, therefore Manufacturing systems need to analyze the product and process control for the measurement of parts to determine geometric errors. The present work develops an analysis on finding translational and angular error parameters of an H-type Gantry system in a laser measurement machine. These parameters cause positioning errors to the 3-axis machine. Different sensors are mounted into the system capable of acquire accelerations, angle orientations and translational positions for constant monitoring of the machine. These sensors are used, along an Articulated Arm Coordinate Measuring Machine (AACMM), to determine error parameters presented in the Gantry system. The recorded data is used to construct an Homogeneous Transformation Matrix of the whole system for finding the deviation in each axis in the machine, especially along the Z-axis. An Inertia measurement unit (IMU) sensor is mounted into the system to find angular errors that can affect the system. The objective is to use this sensor to establish normal parameters of operation for the machine to further develop the digital twin.

## List of Figures

## List of Tables

# Contents

# Chapter 1: Introduction

In the past, there have been cases in which poor quality control has threaten a company's survival. It can happen to any company, even those who are worldwide recognized, such as Toyota and General Motors. From 2009 to 2011, Toyota recalls of millions of vehicles due to sudden acceleration and GM was fined $35 million by the U.S. Department of Transportation (DOT) in 2014 due to vehicles with faulty ignition switches [1]. According to Eifler and Howard, GM ignition switch recall offers a unique possibility to create awareness of early stage robust design and one of the possible causes of the failure might been in the analysis of geometric tolerances [2].

This has caused that clients keeps demanding for higher quality products. Manufacturing systems need to analyze the product and process control for the measurement of parts to determine geometric errors. This is done through a tolerance analysis to find the most probable cause of errors and take actions to reduce possible failures[3].

Dimensional measurements play a key role to guaranty the quality of products. The field of coordinate metrology for Coordinate Measuring Machines (CMM) is based on the interpretation of coordinates in a 3D plane. It has the aim of improving the precision of parts machined by various manufacturing processes. With this, it is also possible to monitor the quality of the process and the prediction of failures.

Since the term of Industry 4.0 was established, digitalization in industries has been transforming the way products are produced. The rise and development of new

information technologies represent new opportunities in the competitive industries, which have brought the term Smart manufacturing [4].

It is known that today's market is highly competitive, and that means that digitalization in manufacturing is an opportunity for companies to achieve high levels of productivity [5] and allow easy integration of interconnected intelligent components inside the shopfloor [6].

What industries seek is to use digitalization to its advantage by creating a data convergence between the physical and the digital world. In order to accomplish this, the term "digital twin" has become a big deal to smart factories for the creation virtual models.

### 1.1 Background

The use of LVDT contact sensors to measure die casting prior to machining are useful for a quick inspection of workpieces, but it also has its limits. A system using LDVTs as gauge tools, are able to determine if a workpiece is between specs. The machine tells the user the workpiece is within tolerances, but it does not provide any further information for analysis. The use of these sensors lack of connectivity, which lead to the development of a new measuring machine in 2017 [7] [8].

The objective was to design a reliable and high precision measuring machine consisting of a laser measuring system, which improved the process and product monitoring, as well as connectivity.

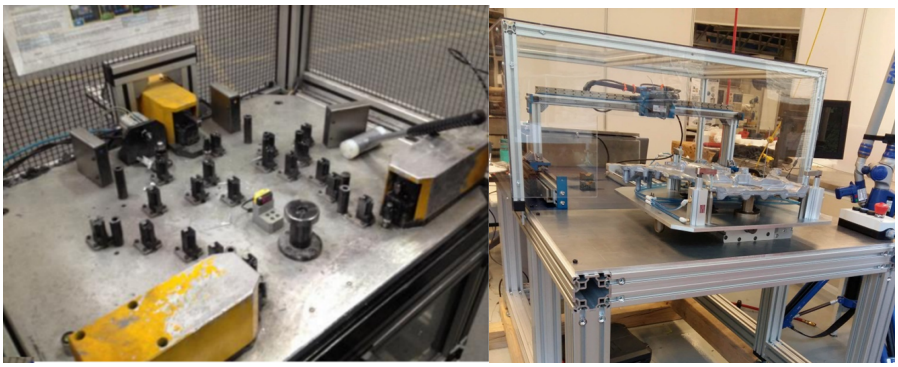

(a) (b)

Figure 1. a) Machine with LDVT b) Machine with a laser sensor.

To assure accuracy, a novel kinematic couplings configuration was developed and tested that allows easy lateral access of the workpiece, which was also verified by various R&R tests.

The shape of the workpiece and the measurement points are shown in Figure 2.

Figure 2. Die-casting part

Table 1. R&R tests

| 13-Dec-17 | |
|---|---|
| Point | %R&R |
| 1 | 6.35 |
| 2 | 3.56 |
| 3 | 3.15 |
| 4 | 3.46 |
| 5 | 3.63 |
| 6 | 2.34 |
| 7 | 2.3 |
| 8 | 2.51 |
| 9 | 2.51 |
| 10 | 2.16 |
| 11 | 2.83 |
| 12 | 3.04 |
| 13 | 3.32 |
| 14 | 4.28 |
| 15 | 3.75 |
| 16 | 3.13 |
| 17 | 3.64 |
| 18 | 4.22 |
| 19 | 3.77 |

| 20-Jun-19 | |
|---|---|
| Point | % R&R |
| 1 | 8.51 |
| 2 | 7.86 |
| 3 | 5.82 |
| 4 | 5.73 |
| 5 | 12.99 |
| 6 | 16.74 |
| 7 | 27.09 |
| 8 | 15.41 |
| 9 | 7.46 |
| 10 | 19.82 |
| 11 | 36.54 |
| 12 | 16.04 |
| 13 | 25.78 |
| 14 | 24.93 |
| 15 | 14.33 |
| 16 | 7.81 |
| 17 | 8.33 |
| 18 | 14.31 |
| 19 | 32.71 |

| 26-Jun-19 | |
|---|---|
| Point | % R&R |
| 1 | 2.33 |
| 2 | 2.45 |
| 3 | 2.33 |
| 4 | 3.01 |
| 5 | 3.33 |
| 6 | 2.43 |
| 7 | 4.04 |
| 8 | 2.12 |
| 9 | 1.96 |
| 10 | 2.52 |
| 11 | 2.68 |
| 12 | 1.94 |
| 13 | 2.44 |
| 14 | 2.16 |
| 15 | 4.44 |
| 16 | 2.10 |
| 17 | 2.20 |
| 18 | 1.84 |
| 19 | 1.83 |

The first R&R test shows results for every point below 7%. The results in all points increased in percentage on the second shown test. This happened because a kinematic coupling fell, as seen in Figure 3.

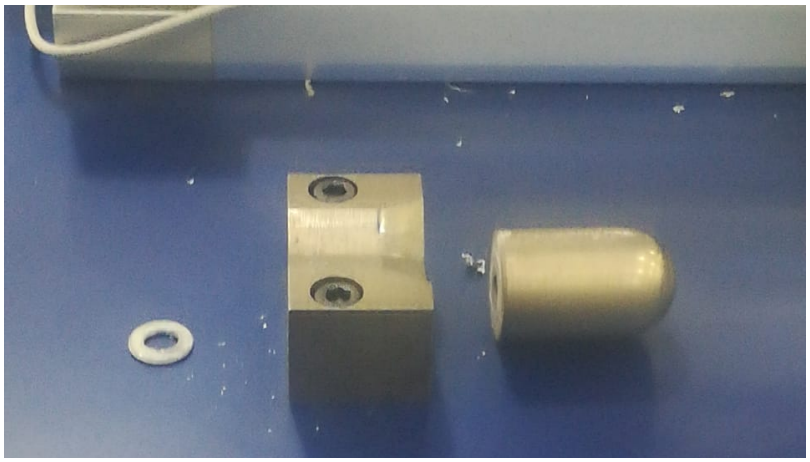

Figure 3. Kinematic coupling

After adjustments were done, the third table shows that accuracy increased. According to the last R&R results, the range points were from 13 to 44 micrometers and tests done with two LDVTs sensors, showed that there are variation errors between 3.1 and 5.1 micrometers, which some of those errors are because of temperature and Hertz contact stresses.

### 1.2 Problem Statement and Context

The gantry system uses permanent magnet synchronous linear motor (PMLSM), which compared to other kind of motors, has both a high control precision and fast dynamic response. That might sound reliable, but the use of PMLSM in parallel cause an inevitable deviation between the two motors, which leads to having translational and angular errors in the system.

Accuracy on the Z-axis is critical for the function of the measuring machine. According to [9], about 70 percent of the inaccuracy of a machine tool is caused by quasi-static errors. It is known that some error in the Z-axis is caused because of the laser repeatability,

temperature and Hertz contact stresses, but they are not the only causes for error in positioning.

There is a need to understand what other factors contribute to the errors of repeatability. In addition, there is a need to monitor the process by receiving feedback from the sensors, the final goal is to predict and prevent machine failure.

### 1.3 Objective

The objective of this work is to identify the sources of error in repeatability of the machine and identify the values of certain parameters that are consistent with the normal operation of the machine. In particular:

To develop the Homogeneous transformation matrices to predict positioning errors by construct inaccuracies (gaps, lack of squareness) and due to acceleration.

To make use of the encoders in the system to determine the positioning error by the effect called “pull and drag” [10].

Design monitoring systems with sensors to obtain machine information to predict failures due to variations in measures along the Z-axis.

Establish contributions of different factors to the variability found in the R&R tests

Use IMU sensors for finding orientation angles to establish normal parameters of operation for the machine.

### 1.4 Design Overview

The solution includes the implementation and use of new sensors in the Gantry system in order to determine positioning errors in different measuring points to establish a normal operation range according to the data obtained from the orientation given by the IMU sensors.

The whole analysis consists of the following:

- A physical machine conformed of an H-type Gantry system that uses 3 PMLSMs.

- Analysis of the positioning error with the use of different sensors and measure machines.
- Measuring the angular and translational errors in the Gantry system.
- Use the homogeneous transformation matrices method to determine errors in position.
- Determine the error with the data obtained directly from the machine.
- Evaluate the system performance according to the results

### 1.5 Research Contribution

Different authors just focus to solve the synchronization problem between parallel motors but do not analyze the whole system errors [11] [12]. The contributions of this work are the implementation and use of new sensors to provide feedback to the user. The recollected data can be used to find quasi-static errors on the machine and set normal operating parameters to predict failures in the Z-axis accuracy. Said parameters can determine if the machine is working properly or machine errors surpass critical conditions.

An IMU sensor was implemented, calibrated and tested to further develop the digital twin. This allows better monitoring of the machine for failure prediction without the necessity of extensive analysis.

This allows a new use of the IMU sensor as an indicator of a possible failure in the machine.

### 1.6 Thesis Organization

The research work is organized into seven chapters, with this section as the first one.

Chapter 2: Contains the literature review of the work. It discusses previous researchers work and description of the methods used and about the methods proposed.

Chapter 3: Describes the sensors and tools used to find the different errors in the system. It explains how they are used for monitoring, failure prediction and corrective actions. The chapter evaluates in certain scenarios and modeling states.

Chapter 4: Explains the Homogeneous transformation matrix method and how it is used to analyze the different errors caused by the machine. The error in the Z-axis and how this is calculated between different measuring points is determined.

Chapter 5: The chapter discusses the experiments done and the obtained results. Presents an analysis of the proposed methods and what do they mean in the operational system.

Chapter 6: It discusses the whole document in a single conclusion of the work done and shows what can be done for the future.

## Chapter 2: Literature review

Advances in technology lead to better manufacturing processes, hence, measuring tools and techniques become more accurate and reliable. As technology, precision engineering keeps growing and leading to greater performance in terms of accuracy.

According to [13], the accuracy of a device is not the only thing to be concerned about when precision engineering is discussed. Other parameters such as the range of motion, environment elements and external disturbances must be taken into consideration too. He considered that the greatest sin in precision machine design is to allow an angular error to manifest in linear systems and declared that it is very important for the design engineer to be able to predict the performance of the system. The author also brought different cases to explain linear and rotation errors. He presented general modeling for predicting these errors. The models were inspired by the principles of rigid bodies kinematic analysis and the Homogeneous Transformation Matrix (HTM) method. The

HTM is a 4x4 matrix, used to represent one coordinate system with respect to another. This is done to estimate volumetric errors [14].

$$HTM(r,p) = \begin{bmatrix} r & p \\ (3x3) & (3x1) \\ 0 \quad 0 \quad 0 & 1 \end{bmatrix} = \begin{bmatrix} r_{11} & r_{12} & r_{13} & X \\ r_{21} & r_{22} & r_{23} & Y \\ r_{31} & r_{32} & r_{33} & Z \\ 0 & 0 & 0 & 1 \end{bmatrix} \quad (1)$$

Where r are the rotating elements in the system and p the translational ones.
Different authors, such as [9] and [15] made an analysis for modeling quasi-static errors in five-axis machines by using the kinematic transformation chain. Both mention temperature, geometric, kinematics and dynamics as sources of errors. The authors based their methods on the rigid body kinematics assumptions, but the difference relies on the machine's structure. [9] found out 52 error parameters in a bed type machine, while [15] found 37 error components in a gantry system. All error parameters are based on how many linear, angular and squareness errors are found.

The HTM method is a series of 4x4 matrices, but [16] goes further to develop a more complex model. The first part of the analysis is a generic HTM error model between coordinate frames based on the forward kinematic method. In the last part of the analysis, a Jacobian 6x6 matrix is obtained by using transforming differential motion axis to compensate for the integrated error components of a grinding wheel. The jacobian matrix is needed if motion errors are considered in the system.

As some structures might require a complex analysis of the system, a simplified approach to measure 21 error parameters is proposed by [17] for three-axis machine tools. The paper introduces the principles and practical applications of a simple testing method using common measurement devices. 21 forms of geometric errors were measured by the use of probes, gauge blocks, and straight gauges. The authors explain the use of each device in a series of steps to find the desired error. Once all parameters are found, the final model is based on a generic HTM. Although the authors explain how to find each error parameter and what type of gauge or probe to use, they do not provide a specific tool or brand to do the measures. The model is also limited to only 3-axis machine tools of similar structure, so it can only be used for similar cases.

Even if the previous authors use similar approaches for positioning error compensation, the model found by each of them ends up being different. Because of the previous statement, [18] proposes a generic kinematic error model to characterize geometric errors of similar gantry systems. According to the authors, extensive research has been made to model geometric and thermal errors of machine tools to find generic models that can be used on similar bridge-type moving gantry machines. The models also consider systems with one and two moving systems. The generic model's objective is to reduce the modeling and implementation efforts, it considers linear, angular and squareness errors.

Many researchers analyze what is known as squareness errors instead of just linear and angular errors. [19] presents one novel model of squareness errors using the Danevit-Hartenberg (DH) parameters for geometric errors to improve the accuracy of machine tools. The DH parameters are the most common and standard way of representing a robot architecture [20]. It considers the motion of the axis and reflects the geometric meaning of the squareness error.

[14] evaluate multi-axis systems characteristics and performance for a laser interferometer-based measurement. The idea of reducing the positioning errors by software-based alternative approaches to providing real-time prediction and correction of geometric and thermally induced errors.

The HTM method is not the only analysis used for determining positioning errors. [11] and [12] do a dynamic analysis of gantry systems. Both authors proposed a dynamic model based on Lagrangian equations to minimize the error caused by the synchronization of dual-drive parallel motors. Instead of a quasi-static analysis, a dynamic analysis is done. This approach analyzes the inertia of different central masses in the system. It is able to obtain position and angular errors through an analysis involving energies in the system. It analyzes the forces caused by the motors, the frictional forces, the speed of each motor, the position and angle to calculate a final dynamic model corresponding to a dual-drive gantry system. The methods are based on the Lagrange equation, and the final dynamic model is very similar, but the matrices that form the model change depending on the system's structure. The dynamic model is then used for control synchronization of both

motors, giving feedback of the actual position and desired position depending on the motor's parameters.

A similar model is proposed by [10], which also used a Lagrangian based method, but the considered gantry system's analysis is different. The authors focus on high-order linear dynamics, as they consider more factors than other researchers. The model considers the two parallel motors as pure rotational flexible joints with lumped rotational spring stiffness, instead of a rigid crossbar. It is a more sophisticated approach, but it has the same objective to develop a synchronization control of both motors in parallel.

Different strategies for finding positioning errors relies on creating a dynamic simulation of the machine's motors. [21] and [22] develops a dynamic model for Permanent Magnet Linear Synchronous Motors (PMLSMs) able to simulate the motor's function. The dynamic model consists of electrical and mechanical sub-models, which means it can simulate the electrical and mechanical components of a motor if the real parameters are inserted in the model.

Different methods are done to reduce or calculate positioning errors. The first approach is to analyze quasi-static errors by the HTM method. The other two methods involve dynamic modeling to develop control synchronization strategies. These strategies focus directly on the machine's control to compensate for the position error of each motor.

Table 2. Brief description of researched methods

| **Method** | **Description** |
|---|---|
| **HTM analysis** | It is used to analyze multi-axis systems to find positioning errors. It measures quasi-static errors on the system to construct a 4x4 HTM that considers translational and angular errors. The positioning errors are found by comparing ideal motion and the constructed matrix. It considers errors in all moving axes. |
| **Lagrangian based dynamic model** | It proposes a serial of Lagrangian based equations that considers the masses, inertia and forces on gantry |

| | |
|---|---|
| | systems. A final dynamic model is constructed for real-time feedback and compensation of the error in position. It is done to compensate the error caused by motors set in parallel but does not make a full analysis of all error parameters. |
| **Dynamic modeling of PMLSM** | Creates a dynamic model using the electrical components of the motors. Creates a simulation of the PMLSM consisting of electrical and mechanical sub-models. The simulation works by inserting the physical system's parameters. It shows the optimal function of the machine but does not considers the errors in the system. |

From the researched methods, the one that analyzes all the error parameters caused by the system, is the use of HTMs. The dynamic modeling ones only focus on the angular and translational errors caused by the desynchronization of dual-drive motors They do not analyze the inclination of the rigid bodies caused by motion. The proposed work's analysis requires of all the possible causes of error in the system, therefore an HTM an analysis is chosen.

# Chapter 3 Data acquisition

The present chapter describes the physical components of the machine and the different sensors used for monitoring. This chapter shows the design of the laser measuring machine and a brief description of its structure. It explains the Gantry positioning system and which sensors are mounted in the system.

Data recollection is needed to monitor the machine, therefore there are different sensors that are being used. These sensors recollect accelerations, measure distances, positions, inclination angles and environmental conditions. This chapter provides general information on these sensors, how they are being used and for what purpose this data is being acquired.

## 3.1 Physical machine

A new non-contact measurement system was developed in 2018 for the inspection die casting workpieces [7] [8]. The current machine CAD model can be observed in Figure 4.

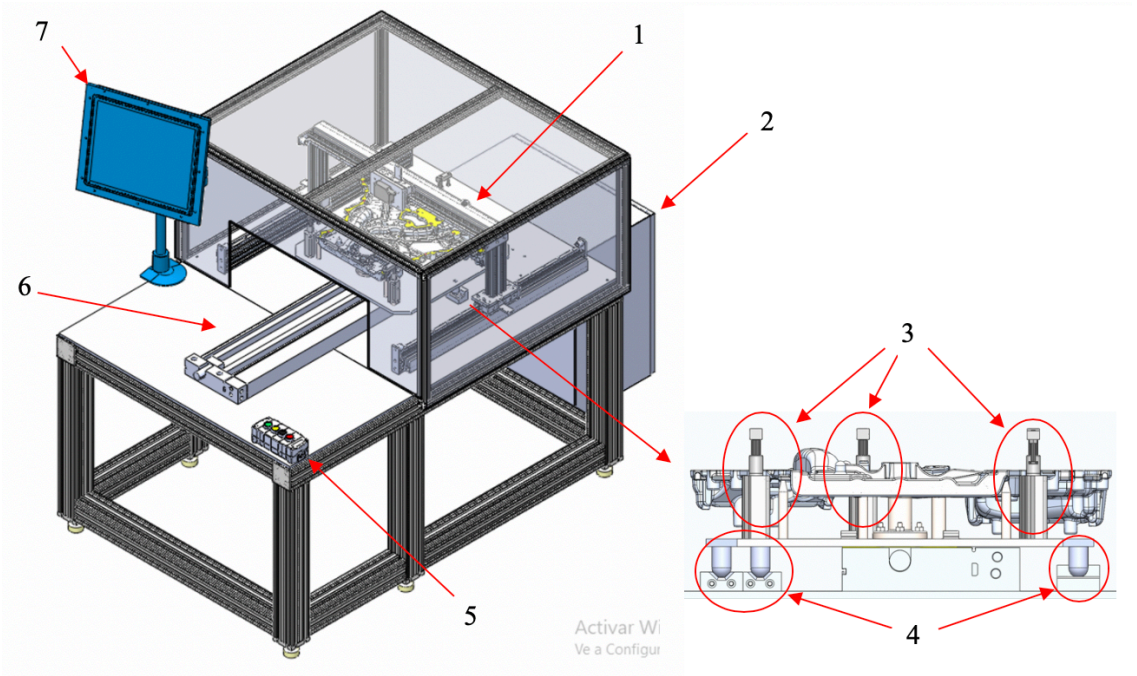


Figure 4. Laser measurement system 1) H-type gantry system 2) Electrical box 3) Fixing system and clamps 4) Control buttons 6) Pneumatic linear actuator 7) Screen

The machine structure was done in a way that it can support a positioning system based in a Gantry H-type system, which was isolated inside a covered area. This protects the system from dust or other residues and external collisions when the gantry starts motion during measurements.

The other elements in the machine are a load/unload mechanism that moves the plate containing the workpiece under the laser sensor that is attached into the upper motor of the gantry system.

The H-type gantry system is the main component of accurate positioning of the laser sensor for measurements. It contains three synchronous linear permanent magnet motors that allow the movement in two different axes, X and Y, that allows the measurement done by the laser in the z-axis. The gantry system can be seen in Figure 5 below:

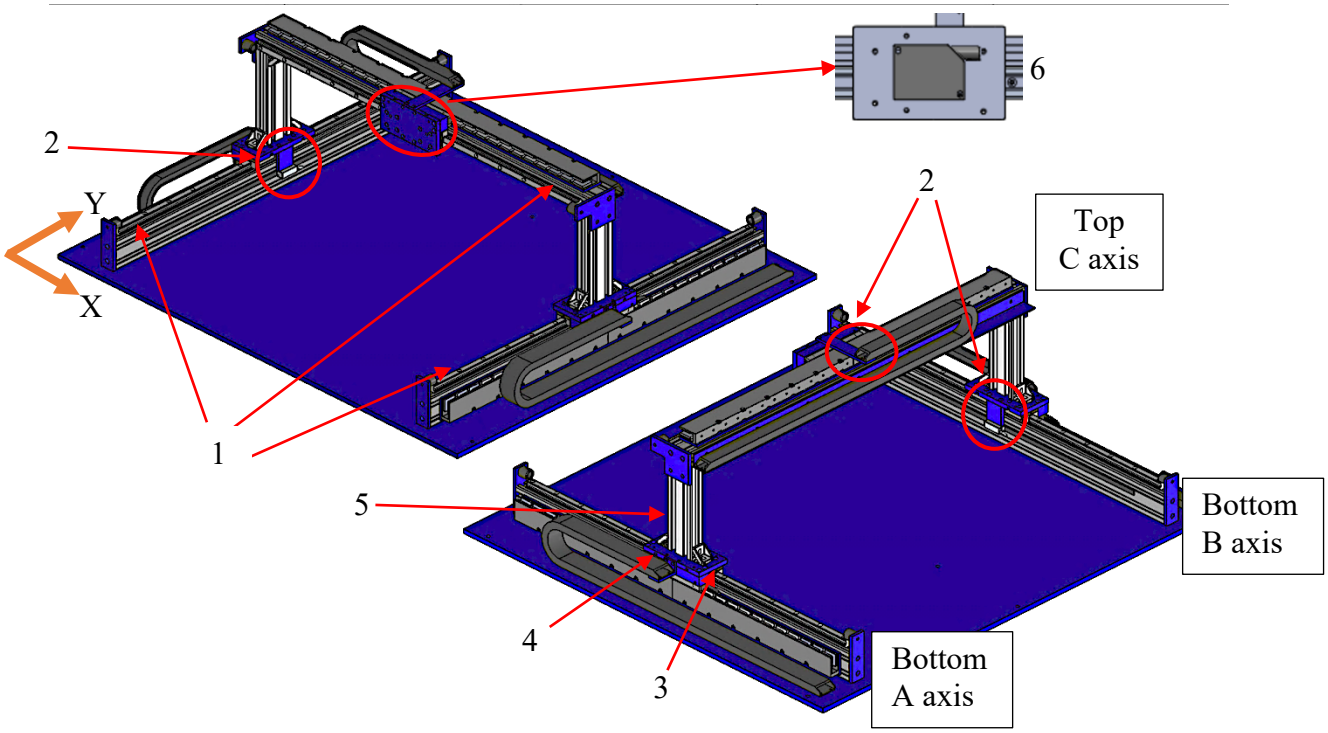


Figure 5. Gantry H-type system 1) Slide rails 2) Encoder sensors 3) Bearing block 4) Motor coil 5) Aluminum frame 6) Laser sensor mounted on the plate

The laser sensor needs a driver por position. The linear motors in the gantry are controlled by a Galil controller that allows the communication of the sensors and other devices on the gantry.

### 3.2 Monitoring

The machine operates using an open-source hardware microcomputer called Beagle Bone Black (BBB).

The industrial version of the BBB is used to communicate with the linear motors in the gantry, send the desired coordinates for the measurements and send information about the machine in both the screen and the cloud.

In general, the BBB is the one that interacts with all the sensors and motors of the machine as is the main device that gives the orders to the machine.

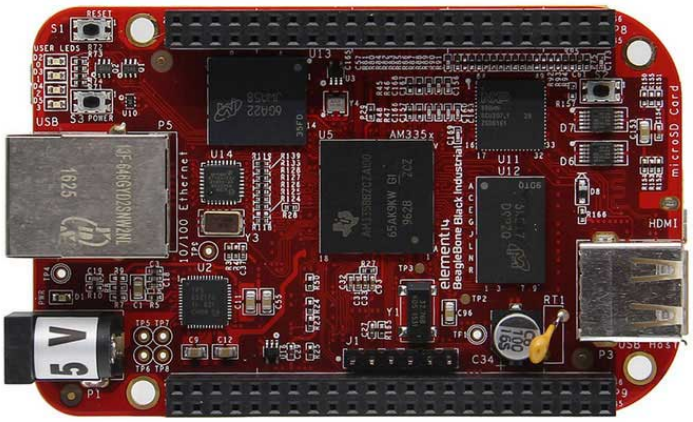


Figure 6. Industrial BBB

As it interacts with the motors' controller, it sends the coordinates of the measurement points. It makes the correct compensation to position the laser on the desired coordinates and set the origin point.

**Laser sensor:**

The laser sensor as a measurement device was selected because of its resolution, error, and measuring speed. Its specifications are shown in
Table *3*.

Table 3. KEYENCE Laser sensor

| | |
|---|---|
| Model | LK-H157 |
| Measurement speed rate | 4KHz |
| Reference distance | 150 mm |
| Range | ±40 mm |
| Repeatability | 0.25 μm |


Figure 7. Laser sensor mounted of the top plate.

This can be considered as the end tool on the gantry system and is the one that needs to be located in specific measuring points.

**Encoders:**

There are three encoders on the system, two on the parallel motors that moves along de Y axis, and one on the top motor on the X axis. The encoder is formed by a magnet track on the stationary part of the motor and the read sensor is mounted on the moving component of the motor, shown in Figure 8.

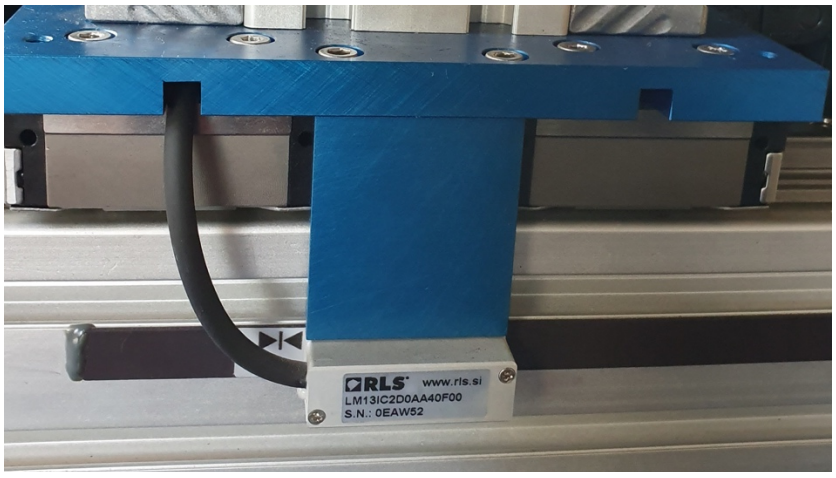


Figure 8. Encoders mounted on the Gantry system.

The encoders give feedback to the machine to establish the commanded position. The position data will be used to obtain the actual position of the machine compared to the desired position and predict angular errors caused by the kinematics of the system.

According to [23], the encoder has a resolution of 1 micron and operates at 500 Hertz.

The encoders are able to take measurements every 2 milliseconds, for a full measurement cycle, the machine takes approximately 4000 measures. This means that it takes almost 8000 milliseconds for one cycle, as it can be seen in Figure 9.

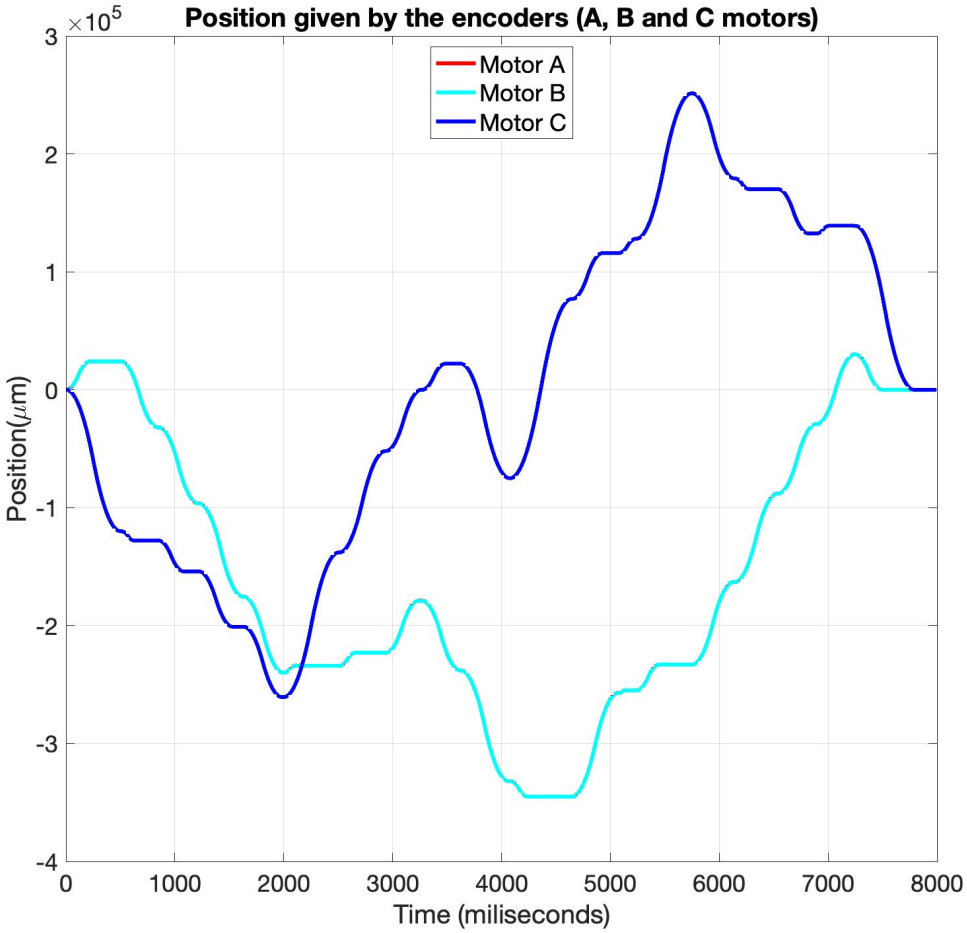


Figure 9. Positions recorded by the encoder in each motor, A, B and C.

Ideally, the motors in parallel, A and B, should be in the same position, however in reality there may be a slight misalignment. In Figure 9, the curve of motor A is not

visible as it is almost the same as B, but as can be sees in , they have a slight difference in micrometers.

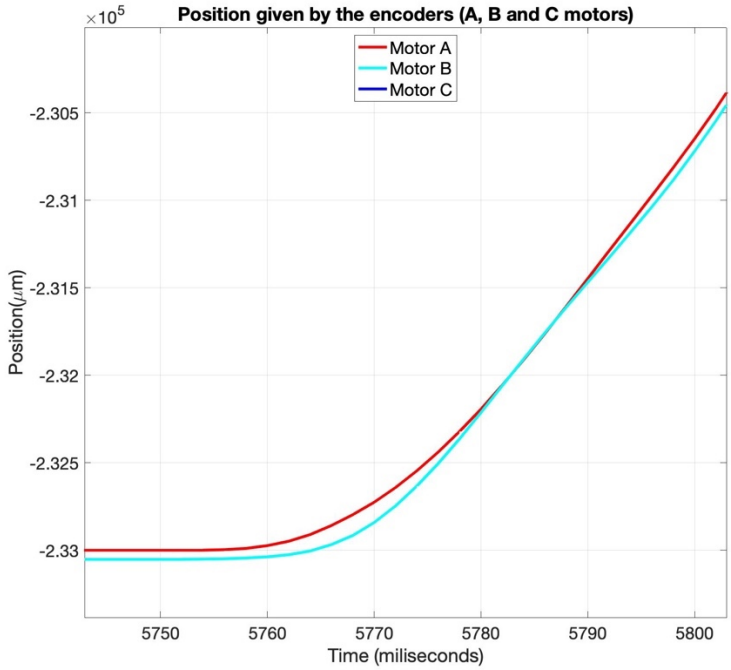


Figure 10. Closer look at the position of motors A and B.

**Galil controller**

The cartesian system includes a Galil controller (Figure 11) to move the motors of the gantry system and locate the laser into the desired position. This controller also has the advantage that allows communication with the laser sensor.


Figure 11. Galil Controller DMC-4143

**MPU 6050**

The MPU 6050 has three types of sensors, it has accelerometers and gyroscopes in three axis, X, Y and Z, and a temperature sensor. Its details can be seen in

.

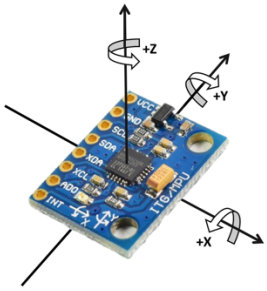


Figure 12. MPU 6050

It is an Inertia measurement unit (IMU) of 6DOF, as it can measure speed, orientation and acceleration in a system. The signal of both the acceleration and the gyroscope can be filtered to measure the orientation of the sensor and avoid noise signals. It also sends signals at 100 Hertz.

This sensor is used to determine the orientation of the Gantry system in the X-axis.

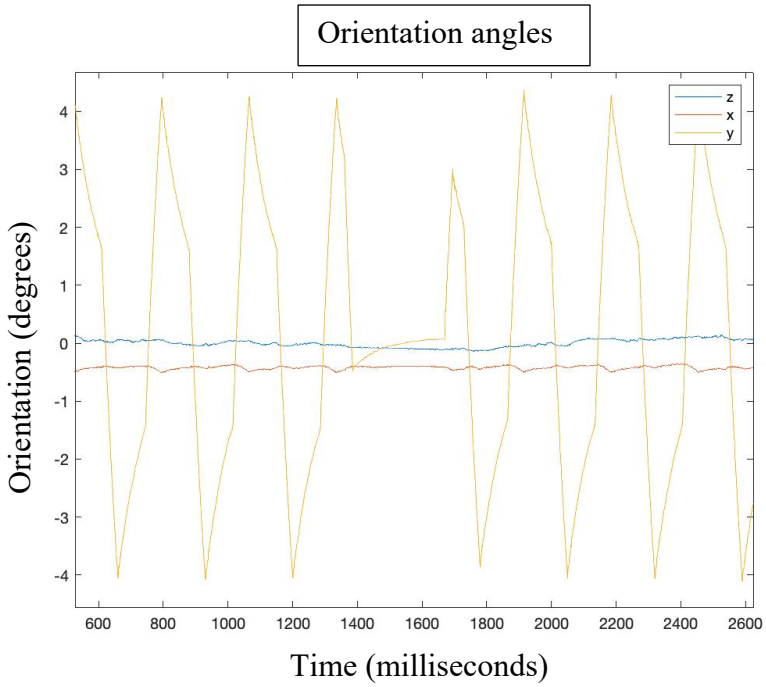


Figure 13. Orientation detected by moving the gantry forward and backward.

### 3.3 Corrective actions

For the moment, sensors are used to monitor the external conditions of the machine, like temperature, pressure, humidity, and dynamic conditions, and acceleration. There are inspection methods to find any disturbances on the machine, such as a higher acceleration than the usual or find a relation between the measured data and temperature.

The present paper looks forward to finding positioning errors caused by dynamic elements, so different models are presented in order to develop a digital twin for monitoring and take corrective actions on the machine. By using the machine sensors and modeled simulations, feedback between the physical machine and the digital twin might prevent or find current errors in the positioning system of the machine.

Once, errors by deviation in the Z-axis are found, they can be compensated in the measurement points. Not only the sensors can monitor and find possible errors in a system, the user or operator can also become a digital thread. Because of that, a manual compensator program for each of the measuring points was added if any of the points has good repeatability and reproduction of the data. A new function was included in the Measurement System to manually configure compensations.

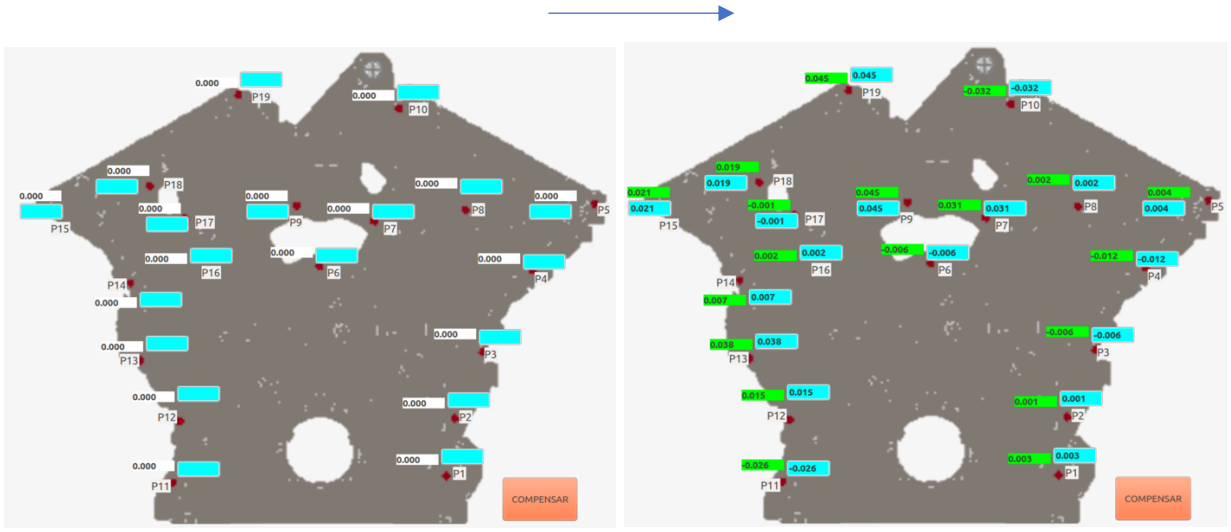


Figure 14. Manual compensation program.

**Quasi-static errors:**

The program is used to set different zeros for each point by compensation, but there is a reason why the Z-axis has deviations in different points. We know that thermal errors exist, but there are also kinematic errors. The FaroArm, an Articulated Arm Coordinate Measuring Machine (AACMM), can be used to measure different points of the system. It was used to find geometric errors in the gantry system, but they are not the only errors to find. To take corrective actions, first it is needed to find the other quasi-static errors, both angular and linear.

As explained before, different sensors were incorporated into the machine to find the linear and angular errors through the system for further analysis and with the use of HTM methods, it is possible to find errors in its three axes, especially in the Z-axis.

The best choice for the error measurement method is to build an accurate and robust predicative model. The combination of the machine sensors provided by the machine can be used as feedback to form a complete HTM analysis for finding the deviation from the ideal positioning and the real position considering errors.

# Chapter 4. Analysis of a dual-drive gantry system

This chapter describes the different error parameters that can be present in the system. It explains why these errors must be considered to analyze the accuracy in the system and how they affect the system. The chapter also explains the use of HTM and the equations used to develop the transformation matrices. It explains the development of a kinematic model and tools and sensors used to find the translational and angular error parameters. This is important to understand the concept of HTM and how it is applied in the positioning error analysis.

## 4.1 Machine errors

Enhancing accuracy in measuring systems is crucial for the manufacturing area, as in precision positioning systems. Errors that can decrease the accuracy of machine tools can be divided into three categories: structurally-induced errors, driver-induced errors, and quasi-static errors [17].

According [9], about 70 percent of the inaccuracy of a machine tool is caused by quasi-static errors.

Although the parallel actuators have the same mechanical structure, the synchronization error is unavoidable due to unbalanced forces that can cause mechanical coupling. It can also happen because of external disturbances to the system. The gantry system has a configuration of machine-slave, which can cause some synchronization problems. To overcome drawbacks, the appropriate approach in the control scheme is by analyzing the dynamic characteristics to satisfy the tracking and synchronization accuracy as the dual-driving stage traces a complex trajectory [12].

The focus is to provide the methodology for the estimation of the geometrical errors of multi-axis machines. Although the machine only moves linearly in two axes, rotational errors must be considered to assure precision. Translational and angular error parameters must be considered in each axis frame. The translational errors are denoted as $\delta_x$, $\delta_y$ and $\delta_z$. Rotational errors are denoted as $\varepsilon_x$, $\varepsilon_y$ and $\varepsilon_z$.

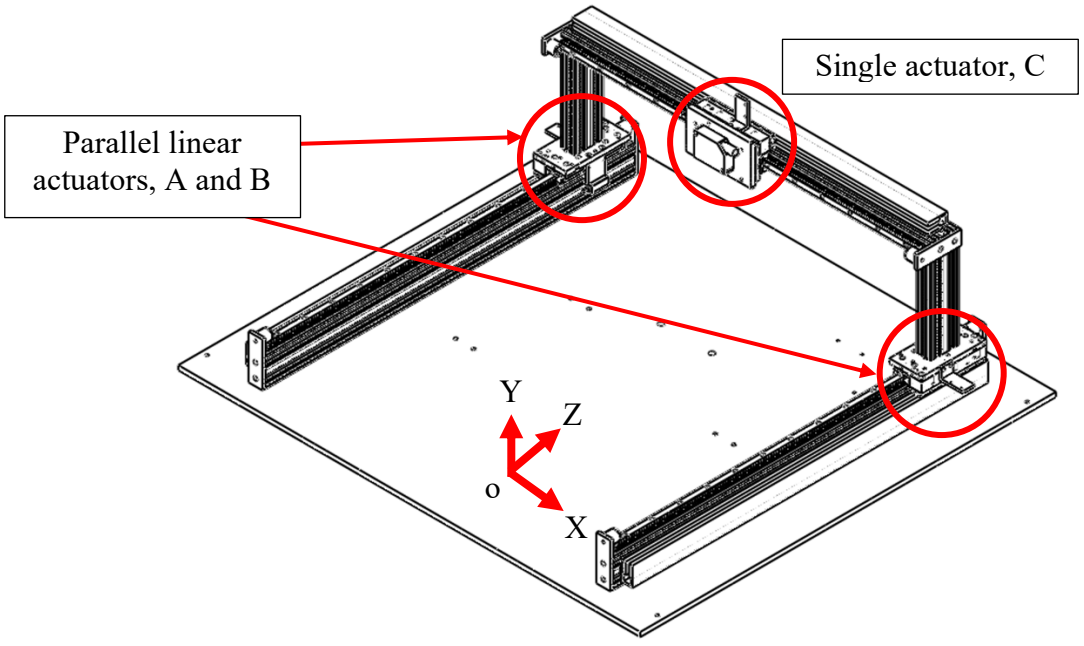


Figure 15. Isometric view of the Gantry system.

Figure 16 shows the top view of the gantry system, as well as its dimensions. It shows the ideal position of the machine, as the crossbeam mounted in the two parallel guidelines is completely horizontal. With a more physics-based model approach we will address the complex dynamic coupling issues.

In this approach, the focus is to find the total angular error is along the Z-axis. Figure 18 shows a clearer example of these errors, noted as $\varepsilon_z$.

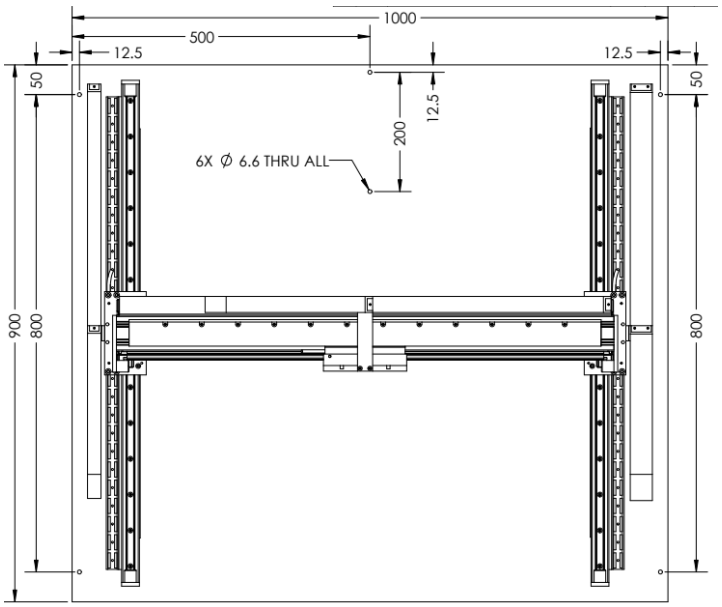


Figure 16. Gantry system dimensions and upper view [8].

The next objective is to find the angular error along the X-axis, as it can create some positioning issues. This error can be seen in Figure 17 as $\varepsilon_x$.

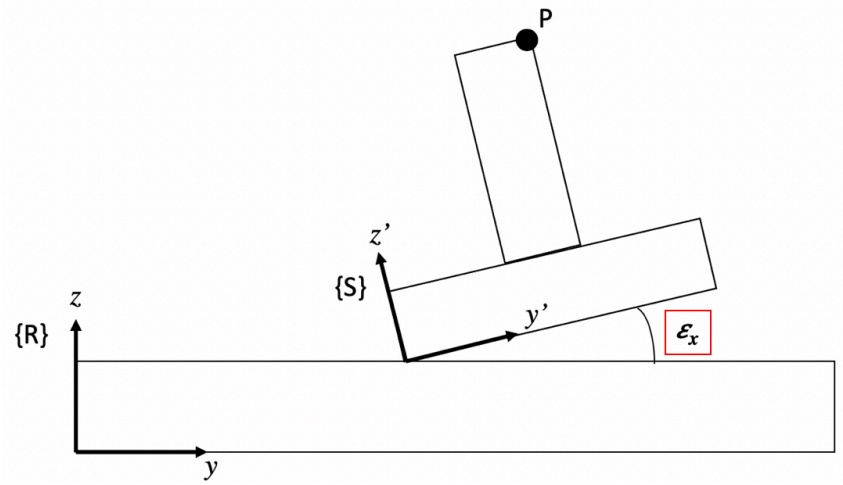


Figure 17. Angular error in axis X

### 4.2 Analysis of the gantry stage

The schematic top view of the H-type gantry is shown in Figure 18. Two linear guides, A and B, are aligned in parallel and a crossbeam, C, is mounted across them. The laser sensor moves along the crossbeam on the X axis direction, while the linear motors moves along the Y-axis. As in this part, we will focus on finding the angular deviation on the Z-axis, for simplicity the head is assumed as rigidly attached to the crossbeam [10].

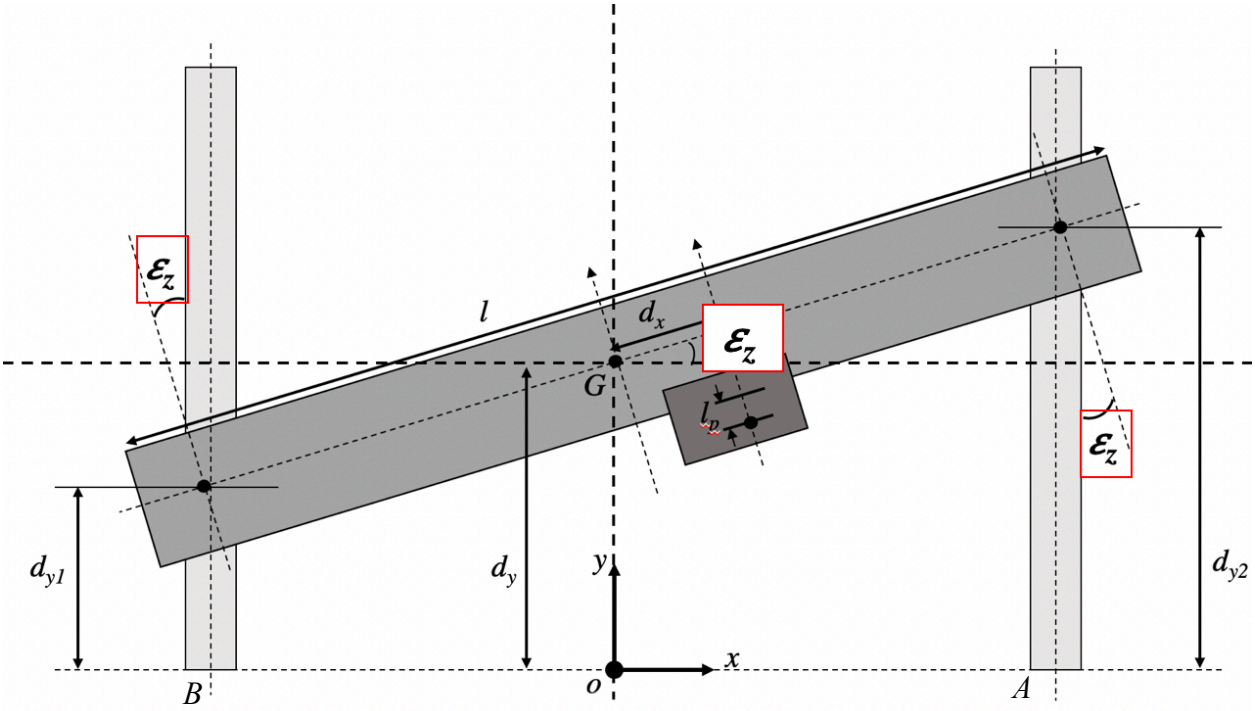


Figure 18. Motion and dynamics of the whole rigid body

The frame $o_{xy}$ is the fixed inertia coordinate frame with origin at the midpoint between the guiderails A and B. Displacements are inevitable since the two actuators might have unbalanced forces, variations in its mechanism assembly, or external disturbances, such as vibrations during working process. Furthermore, G is the center point and the mass center of the entire rigid moving body through the X-axis. This includes the slider and the inspection tool mounted. Because of the deviation between $d_{y1}$ and $d_{y2}$. The gantry also rotates about its center point G and is shown as a rotating angle $\varepsilon_z$.

### 4.2.1 Homogeneous Transformation Matrix

The advantage of using HTM, in general, is that it can show both translational and rotational transformation into a single matrix. However, the HTM assumes rigid bodies, and therefore, the errors associated with the deformation of a link must be accounted for with possible errors [24].

To develop the error budget, it is needed to do a kinematic model of a proposed system, in this case, the laser measurement system, by forming a series of HTMs. Then, an analysis of each type of error in the system and implement these into the HTM model to determine the effect that the errors cause on the end tool (the laser tip) position accuracy with respect to the workpiece's points.

The HTM is a 4x4 matrix and is used for mapping a vector in a homogeneous coordinate from one frame to another in a compact matrix. The matrix is conformed of a 3x3 submatrix that contains the orientation or rotational part of the transformation and a 3x1 submatrix that represents the positional or translational components, as shown in equation 2.

$$T(R,p) = \begin{bmatrix} R & p \\ (3x3) & (3x1) \\ 0 \quad 0 \quad 0 & 1 \end{bmatrix} \tag{2}$$

For ideal translation motions in X, Y, or Z axes, the HTM in each coordinate frame is given in equation 3.

$$T_{p(x,y,z)} = \begin{bmatrix} 1 & 0 & 0 & X \\ 0 & 1 & 0 & 0 \\ 0 & 0 & 1 & 0 \\ 0 & 0 & 0 & 1 \end{bmatrix} or \begin{bmatrix} 1 & 0 & 0 & 0 \\ 0 & 1 & 0 & Y \\ 0 & 0 & 1 & 0 \\ 0 & 0 & 0 & 1 \end{bmatrix} or \begin{bmatrix} 1 & 0 & 0 & 0 \\ 0 & 1 & 0 & 0 \\ 0 & 0 & 1 & Z \\ 0 & 0 & 0 & 1 \end{bmatrix} \tag{3}$$

The corresponding HTM for ideal rotation by an angle $\theta$ in X, Y, or Z axes is shown in equation 4.

$$T_{r(x,y,z)} = \begin{bmatrix} 1 & 0 & 0 & 0 \\ 0 & cos\,\theta_x & -sin\,\theta_x & 0 \\ 0 & sin\,\theta_x & cos\,\theta_x & 0 \\ 0 & 0 & 0 & 1 \end{bmatrix} or \begin{bmatrix} cos\,\theta_y & 0 & sin\,\theta_y & 0 \\ 0 & 1 & 0 & 0 \\ -sin\,\theta_y & 0 & cos\,\theta_y & 0 \\ 0 & 0 & 0 & 1 \end{bmatrix}$$

$$or \begin{bmatrix} cos\,\theta_z & -sin\,\theta_z & 0 & 0 \\ sin\,\theta_z & cos\,\theta_z & 0 & 0 \\ 0 & 0 & 1 & 0 \\ 0 & 0 & 0 & 1 \end{bmatrix} \quad (4)$$

Because the Gantry system only has linear movements in X and Y axes, It is only needed to use the translational transformation matrices, however, errors must be considered.

Equations 2 to 4 are used to find a general transformation matrix. The transformation matrix is be the product of all translational and rotational matrices, which results into equation 5.

$$T_{r(x,y,z)} = \begin{bmatrix} C\varepsilon_y C\varepsilon_z & -C\varepsilon_y S\varepsilon_z & S\varepsilon_y & \delta_x \\ S\varepsilon_x S\varepsilon_y C\varepsilon_z + C\varepsilon_x S\varepsilon_z & C\varepsilon_x C\varepsilon_z - S\varepsilon_x S\varepsilon_y S\varepsilon_z & -S\varepsilon_x C\varepsilon_y & \delta_y \\ -C\varepsilon_x S\varepsilon_y C\varepsilon_z + S\varepsilon_x S\varepsilon_z & S\varepsilon_x C\varepsilon_z + C\varepsilon_x S\varepsilon_y S\varepsilon_z & C\varepsilon_x C\varepsilon_y & \delta_z \\ 0 & 0 & 0 & 1 \end{bmatrix} \quad (5)$$

Where C=cos, S=sin and angles $\theta$ are substituted by $\varepsilon$ to denote error angles.

All rigid bodies have three error values noted as $\delta_x$, $\delta_y$ and $\delta_z$ that correspond to the linear positioning errors, and another three error values noted as $\varepsilon_x$, $\varepsilon_y$ and $\varepsilon_z$ that correspond to the roll, pitch and yaw error.

$$T_i = \begin{bmatrix} 1 & -\varepsilon_z & \varepsilon_y & a+\delta_x \\ \varepsilon_z & 1 & -\varepsilon_x & \delta_y \\ -\varepsilon_y & \varepsilon_x & 1 & \delta_z \\ 0 & 0 & 0 & 1 \end{bmatrix} \quad (6)$$

Angle errors $\varepsilon_x$, $\varepsilon_y$ and $\varepsilon_z$ are negligible and small-angle approximations, so cos $\varepsilon$ = 1 and sin $\varepsilon$ = 0 [13]. *a* is the distance desired for the carrier on the slide.

### 4.2.2 Kinematic model

The laser measurement machine has two translational axes, which are used to adjust the laser sensor tip directly above each of the workpieces desired points to measure. The accuracy of the whole kinematic chain in the machine tool, the laser, can have a direct influence on the measurement precision. Therefore it is desired to establish a relationship between the errors in the components of the kinematic chain and the resulting position and orientation of the tool [15].

As mentioned before, the machine's main focus is the positioning system, which is an H-type gantry system that moves in two axes. The gantry moves linearly along the Y-axis direction while the laser is mounted along the X-axis direction. There is no movement along the Z-axis, but the laser does its measurement through that axis. Figure 19 shows the direction of the moving axes.

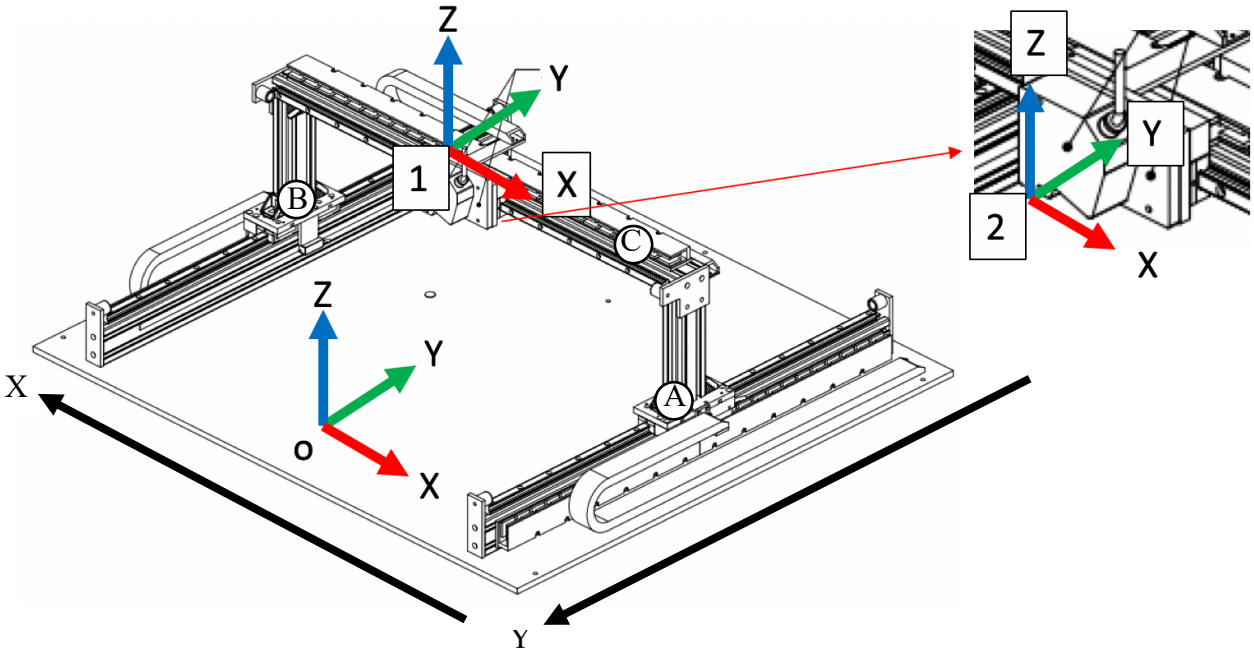


Figure 19. Configuration and coordinate system of the H-type gantry system.

In order to find the transformation matrix for the whole system, first it is needed to find the transformation in each coordinate system.

It is needed to find the kinematic error models for each axis and end tool offset, which is the laser tip, therefore equations 7 and 8 show the transformation matrices.

$$T_1 = \begin{bmatrix} 1 & -\varepsilon_z & \varepsilon_y & X+\delta_x \\ \varepsilon_z & 1 & -\varepsilon_x & Y+\delta_y \\ -\varepsilon_y & \varepsilon_x & 1 & Z+\delta_z \\ 0 & 0 & 0 & 1 \end{bmatrix} \quad (7)$$

$$T_2 = \begin{bmatrix} 1 & 0 & 0 & Xl \\ 0 & 1 & -\varepsilon_x & Yl \\ 0 & \varepsilon_x & 1 & Zl \\ 0 & 0 & 0 & 1 \end{bmatrix} \quad (8)$$

Where $T_1$ and $T_2$ are the transformation matrices in the two proposed axis frames. Therefore, according to the machine kinematic chain:

$$HTM_{system} = T_1 \cdot T_2 \quad (9)$$

The real location of the laser tip is found by multiplying the previous equation and a vector with the desired position,

$$P_{real} = HTM_{system} * P_i \quad (10)$$

So, he positions error is

$$P_{error} = P_{real} - P_{ideal} \quad (11)$$

$P_i$ is the vector position of each one of the points and $P_{ideal}$ is the desired position to reach without considering errors.

### 4.2.3 Error parameters.

Three reference frames were proposed for the HTM analysis. The first one is in origin, the second one on the plate holding the laser sensor, and the last one is on the tools end, the laser's tip. In the last two frames, there will be errors that must be found to fill the transformation matrix on each frame.

**Geometric errors:**

There can be errors driven by the same multi-axis system geometry. In an ideal model, there would be just translational movement in three-axis linear systems, but in real applications, there will be errors that must be considerate. These systems are composed

of a sequence of structural elements connected by joints that provide translational motion, and the more complicated the system is, it can generate more errors.

For determining possible errors in the gantry system, the system was measured using a FaroArm.

The FaroArm is a CMM with a flexible arm operated manually for quality inspection. It will be used to generate a plane on the gantry and measure its height at different points and positions, to determine geometric errors.

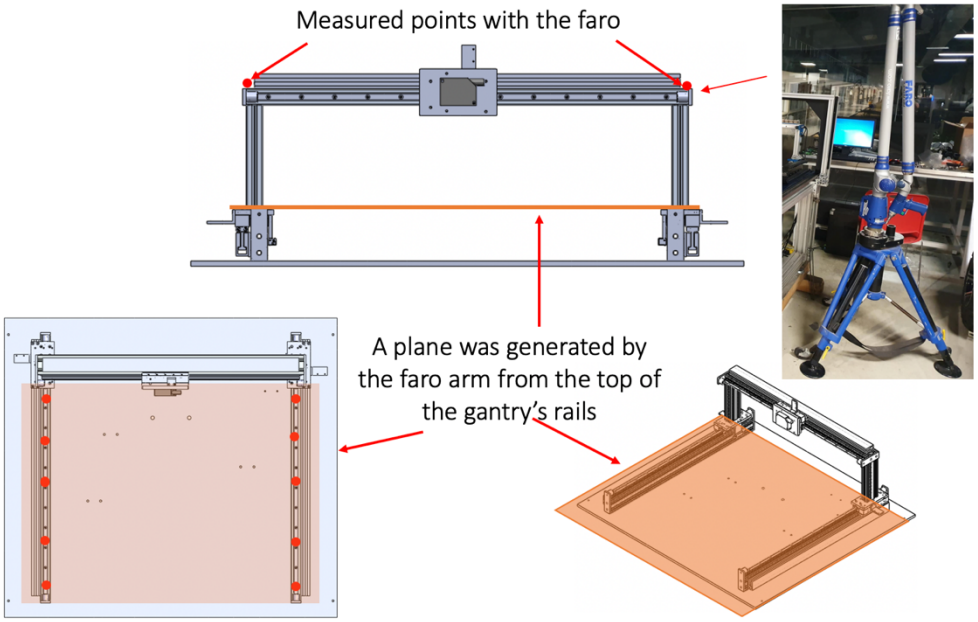


Figure 20. FaroArm application

The top of the Gantry was measured through selective positions sent by the Galil control and encoders to verify position. To verify the variation of the top plane of the gantry, Matlab was used with the data obtained from the FaroArm.

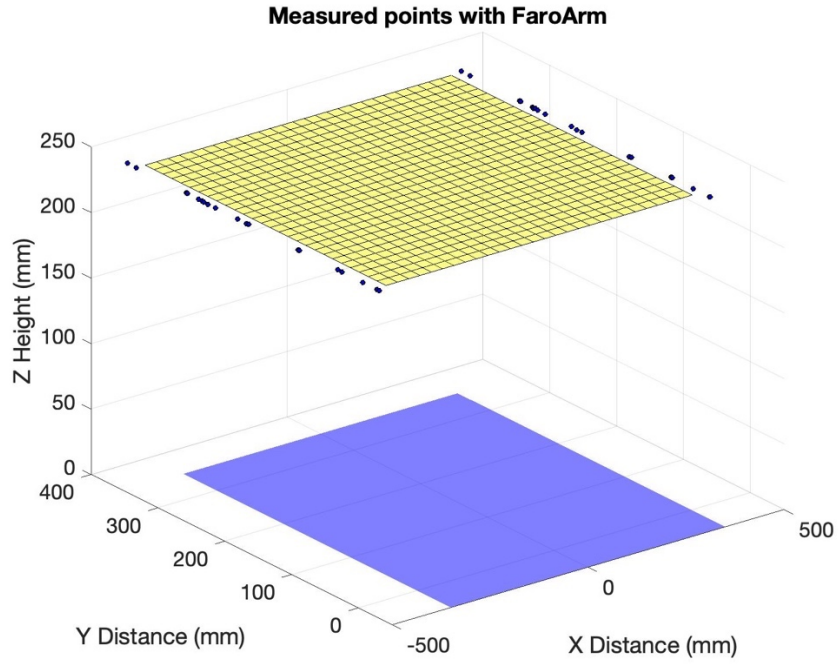


Figure 21. Plane and generated surface of measured points with the FaroArm

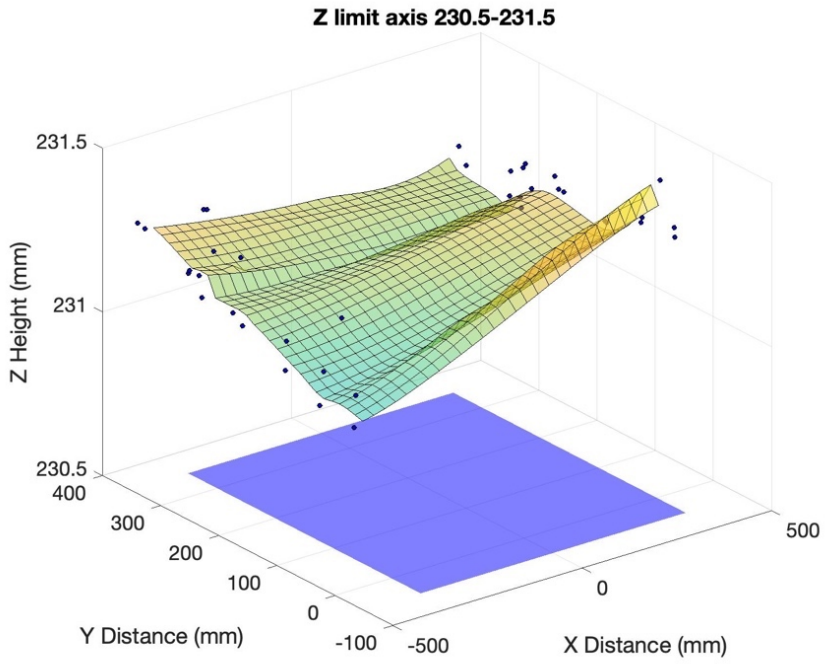


Figure 22. Magnification of the generated surface

As seen in Figure 21, the top of the Gantry is not a perfect plane, hence the system has different geometric errors along different measuring points.

This analysis is done in order to find the angular error in the y axis ($\varepsilon_y$).

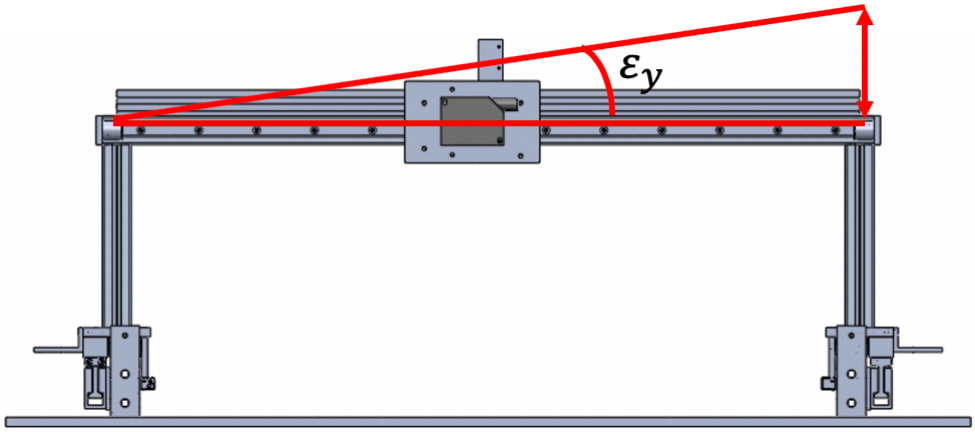


Figure 23. Angular error along the Y axis

It is not the only error to find with the FaroArm, there is also a translational deviation on the z axis ($\delta z$).

This time, the FaroArm measures a set of 18 specific positions. The first step is to set the coordinates to the Galil controller to move the laser sensor in each one of the 18 measurement points.

In each one of those points, a measurement with the arm tool will be made and recorded. This can give information about how the position of the laser's tip changes along the Z-axis and being able to find a deviation in height.

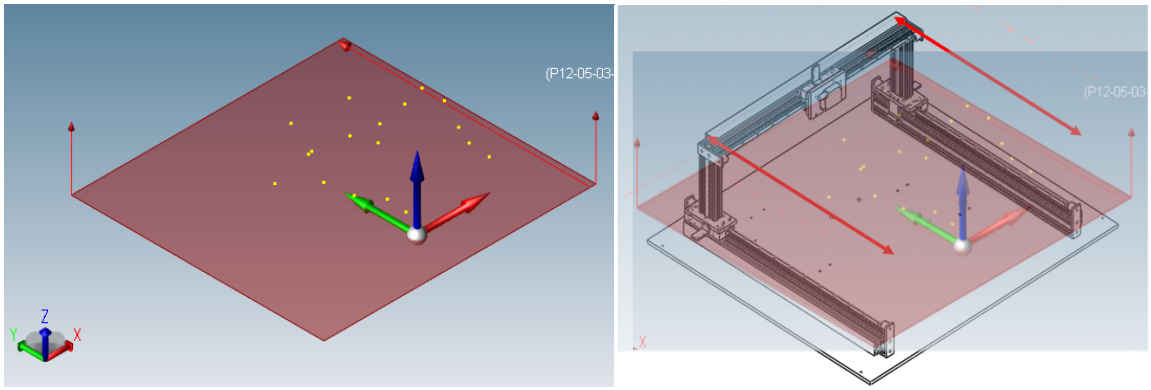

Figure 24. Plane and generated points made by the FaroArm.

The recorded distances of each one of the 18 measuring points are shown in Table 4.

Table 4. Distances in the Z-axis from the plane.

| Feature | z |
|---|---|
| p1 | 205.12 |
| p2 | 205.121 |
| p3 | 205.127 |
| p4 | 205.137 |
| p5 | 205.177 |
| p6 | 205.121 |
| p7 | 205.068 |
| p8 | 205.017 |
| p9 | 204.979 |
| p10 | 205.013 |
| p11 | 205.019 |
| p12 | 205.005 |
| p13 | 205.002 |
| p14 | 205.017 |
| p15 | 204.97 |
| p16 | 204.99 |
| p17 | 204.952 |
| p18 | 204.904 |

The previous analysis was to find the linear and angular errors of the first frame. For the second frame, two planes are generated by the FaroArm to measure the angular error in the X axis:

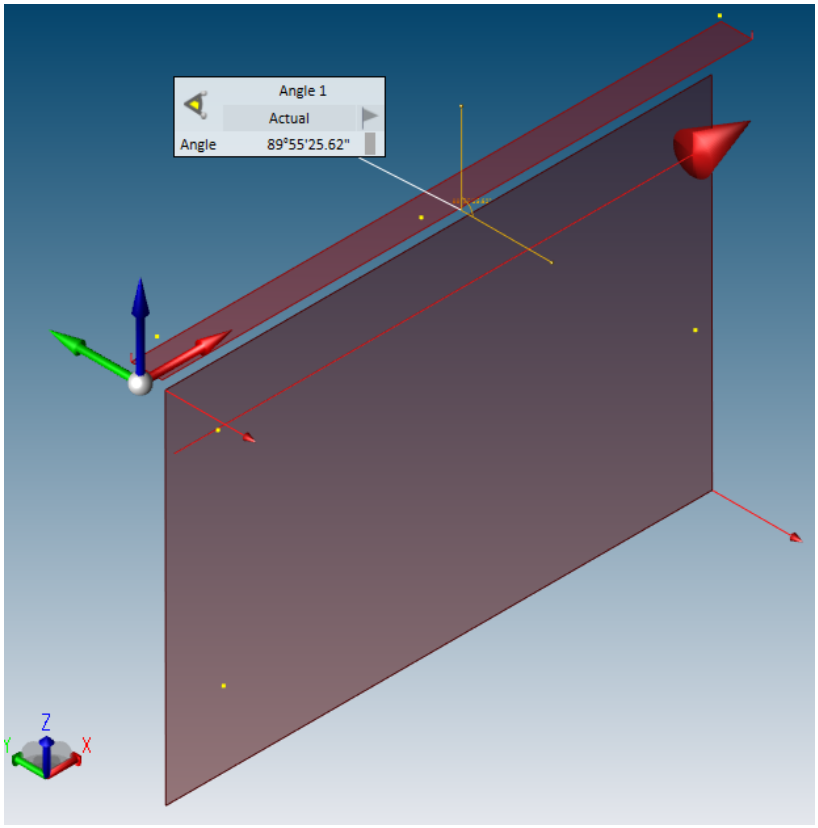


Figure 25. Second frame analysis

**Kinematic errors:**

Linear and angular errors will be caused by the machine's motion. To find these errors, different sensors will be used, the encoders and an IMU sensor.

The encoders are used to find the linear deviation align the Y axis ($\delta_y$) and the angular error in the Z axis ($\varepsilon_z$).

A comparison between the positions will be done to find the differences in positions. Similar to the analysis done with the FaroArm, the errors are in 18 specific positions. Both translational and angular errors will be recorded for implementing the final HTM analysis.

Table 5. All measures are in micrometers

| Position | dy1 | dy2 |
|---|---|---|
| 1 | 24002 | 23946 |
| 2 | -31622 | -31682 |
| 3 | -96424 | -96464 |
| 4 | -175430 | -175480 |
| 5 | -239958 | -240009 |
| 6 | -234000 | -234052 |
| 7 | -222919 | -222983 |
| 8 | -179065 | -179097 |
| 9 | -237910 | -237975 |
| 10 | -331955 | -332026 |
| 11 | -344921 | -345013 |
| 12 | -257007 | -257040 |
| 13 | -254990 | -255053 |
| 14 | -233000 | -233052 |
| 15 | -163161 | -163217 |
| 16 | -88009 | -88062 |
| 17 | -29062 | -29097 |
| 18 | 30017 | 29983 |

The last test is done by implementing the IMU, MPU6050, in the gantry to observe angular errors along the X-axis ($\varepsilon_x$). The IMU has a 3DOF accelerometer and gyroscope, which can be setup to give orientation angles. By filtering the signals given by the accelerometer and gyroscope, one can use the IMU to register when the machine orientation changes. This is done in order to find the angular error in X.

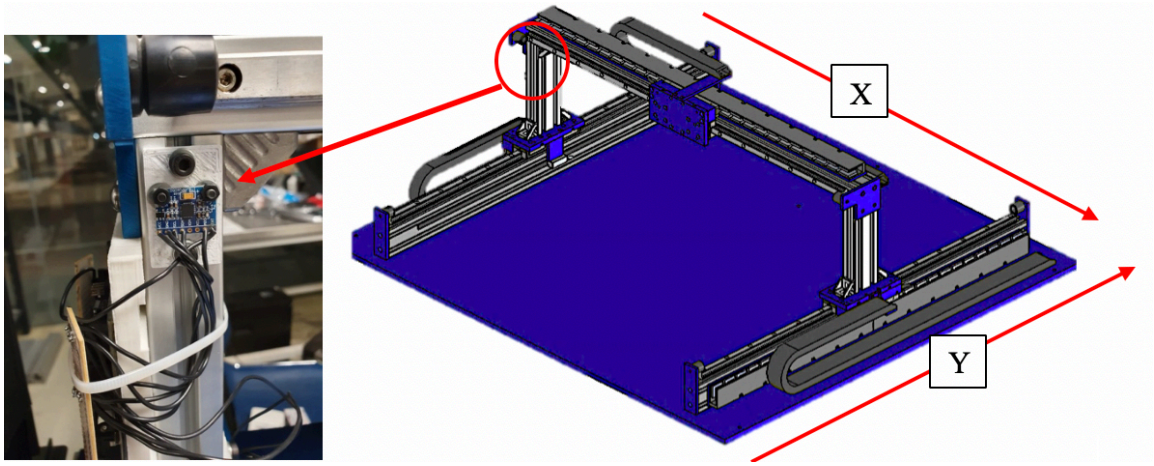


Figure 26. MPU 6050 location in the Gantry.

Once all the error parameters are found, the HTM final matrix is used to find the end effector tool deviation error in X, Y and Z axes.

The MPU 6050 is connected to an Arduino UNO board. The Aurduino UNO is a microcontroller board with digital input and output pins, of which some can be used as PWM, and analog pins. Figure shows how the MPU 6050 is connected.

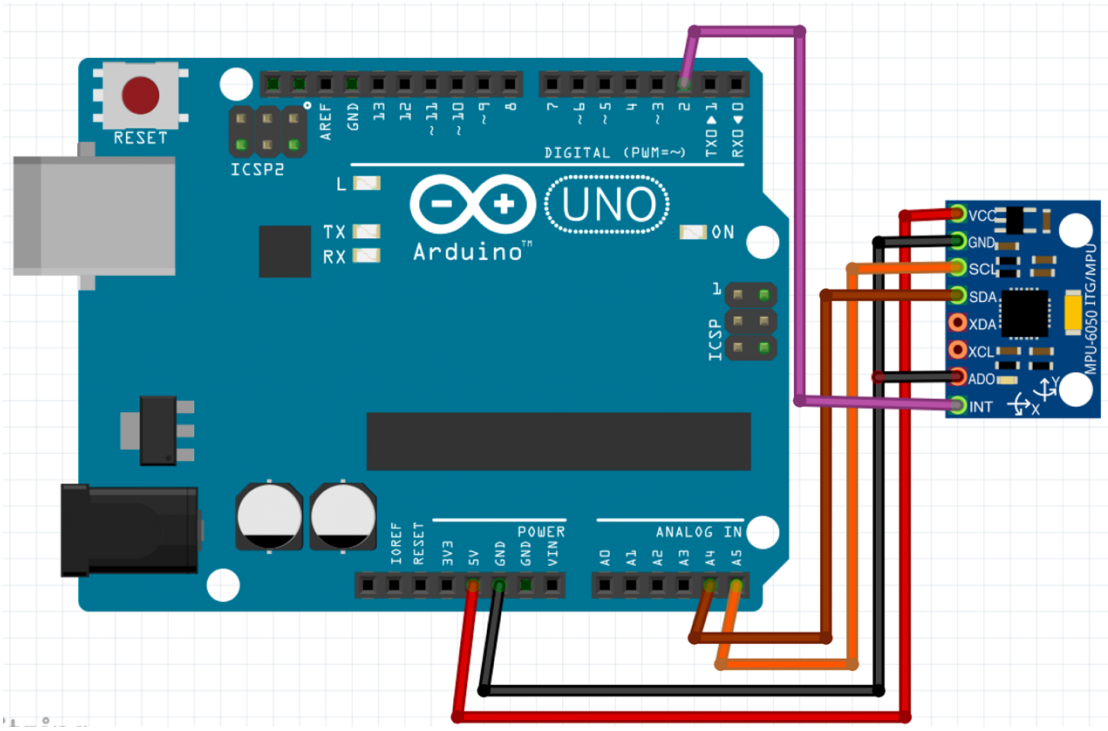


Figure 27. Arduino UNO and MPU 6050 connection.

## Chapter 5: Test, Analysis and Results

The present chapter describes the procedure followed and the data acquired by the different sensors in the machine. It shows the results obtained from the encoders, IMU sensor and the use of the FaroArm.

The chapter shows the transformation matrices used in the different frames and the final equations used to obtain the final deviations in the machine. It also has a final discussion about the obtained data and the prior known errors.

### 5.1 Error parameters

For the analysis of the HTM, different frames are analyzed in the system. To determine the tool's desired position, transformation matrices are created for each frame. To obtain the combined HTM, the multiplication of all the HTMs needs to be done.

The first transformation matrix [T1] can be obtained by analyzing the encoders, the orientation from the MPU 6050 and the geometric errors measured from the FaroArm.

### 5.1.1 Errors found by the encoders

A set of 18 points (Figure 8) were selected to test the HTM model to verify the value of the distance errors in X, Y and Z axes.

First, errors associated with the Y-axis are calculated using the data from the encoders.

The position according to the encoder of Motor A and B are listed in Table 6:

Table 6. Position of motors A and B along the Y-axis.

| Position | dy1 | dy2 | $\delta$y | εz |
|---|---|---|---|---|
| 1 | 24002 | 23946 | 28 | 6.74699E-05 |
| 2 | -31622 | -31682 | 30 | 7.22892E-05 |
| 3 | -96424 | -96464 | 20 | 4.81928E-05 |
| 4 | -175430 | -175480 | 25 | 6.0241E-05 |
| 5 | -239958 | -240009 | 25.5 | 6.14458E-05 |
| 6 | -234000 | -234052 | 26 | 6.26506E-05 |
| 7 | -222919 | -222983 | 32 | 7.71084E-05 |
| 8 | -179065 | -179097 | 16 | 3.85542E-05 |
| 9 | -237910 | -237975 | 32.5 | 7.83133E-05 |
| 10 | -331955 | -332026 | 35.5 | 8.55422E-05 |
| 11 | -344921 | -345013 | 46 | 0.000110843 |
| 12 | -257007 | -257040 | 16.5 | 3.9759E-05 |
| 13 | -254990 | -255053 | 31.5 | 7.59036E-05 |
| 14 | -233000 | -233052 | 26 | 6.26506E-05 |
| 15 | -163161 | -163217 | 28 | 6.74699E-05 |
| 16 | -88009 | -88062 | 26.5 | 6.38554E-05 |
| 17 | -29062 | -29097 | 17.5 | 4.21687E-05 |
| 18 | 30017 | 29983 | 17 | 4.09639E-05 |

The values of $\delta_y$ and $\boldsymbol{\varepsilon}_z$ were found by using the following formulas:

$$\delta_y = \frac{dy_1 - dy_2}{2} \quad (12)$$

$$\varepsilon_z = \frac{dy_1 - dy_2}{l} \quad (13)$$

Where $l$ = 830 mm.

### 5.1.2 Errors found by the IMU:

10 tests were done to determine the maximum angular error in each measurement point. The 18 angle errors can be seen in Table 7. The IMU is used to determine the angular error along the X-axis ($\varepsilon_x$).

Table 7. Orientation in the X-axis

| Position | Time (ms) | Orientation (degrees) |
|---|---|---|
| 1 | 507 | 0.03 |
| 2 | 828 | 0.02 |
| 3 | 1207 | 0.03 |
| 4 | 1627 | 0.02 |
| 5 | 1997 | 0.04 |
| 6 | 2507 | 0.02 |
| 7 | 2977 | 0.01 |
| 8 | 3277 | 0.03 |
| 9 | 3636 | 0.03 |
| 10 | 4136 | 0.01 |
| 11 | 4716 | 0.01 |
| 12 | 5076 | 0.01 |
| 13 | 5246 | 0.01 |
| 14 | 5756 | 0.01 |
| 15 | 6115 | 0.01 |
| 16 | 6556 | 0.02 |
| 17 | 6895 | 0.01 |
| 18 | 7245 | 0.03 |

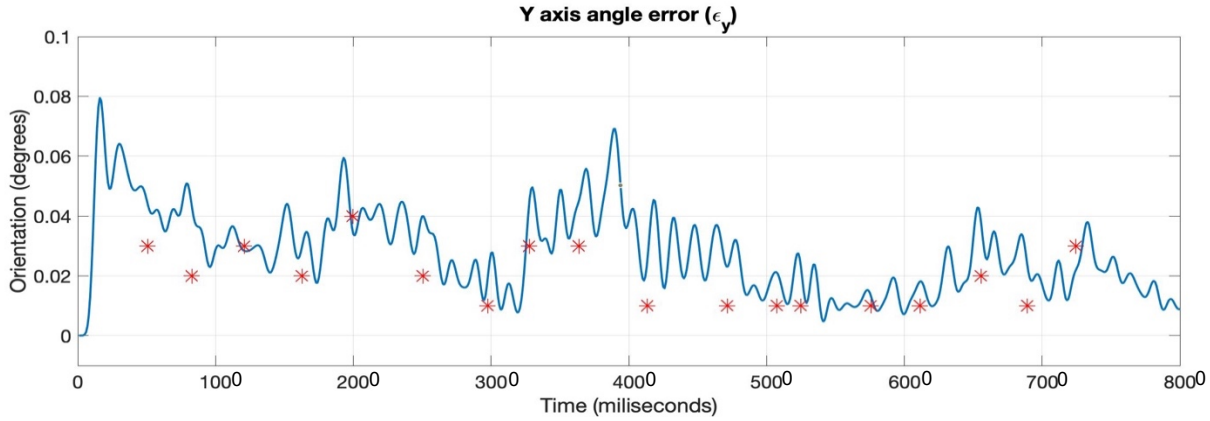


Figure 28. Orientation through time

### 5.1.3 Errors found by the FaroArm:

The FaroArm was used to measure the top extremes of the gantry. The Gantry system was positioned in 18 different positions and in each position, two measures were done. The heights of both the top right and top left of the Gantry system is shown in Table 8.

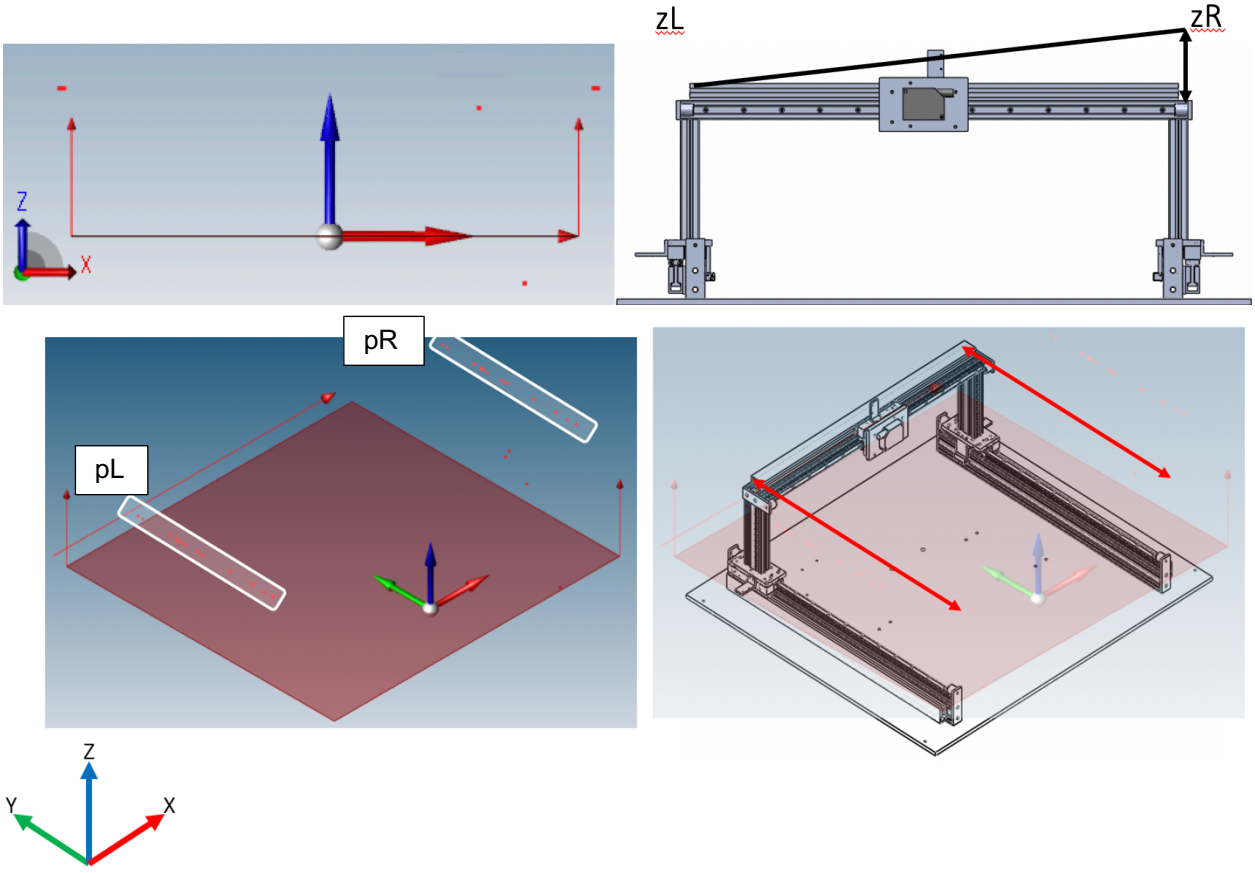


Figure 29. Plane generated and points measured with the FaroArm

Table 8. Measured points coordinate with the FaroArm

| Point | z | Point | z | $\varepsilon_y$ |
|---|---|---|---|---|
| **pL0** | 231.284 | **pR0** | 231.418 | 0.00016101 |
| **pL1** | 231.069 | **pR1** | 231.295 | 0.00027155 |
| **pL2** | 231.091 | **pR2** | 231.274 | 0.00021989 |
| **pL3** | 231.124 | **pR3** | 231.205 | 9.7327E-05 |
| **pL4** | 231.307 | **pR4** | 231.229 | 9.3742E-05 |
| **pL5** | 231.394 | **pR5** | 231.112 | 0.00033899 |
| **pL6** | 231.399 | **pR6** | 231.252 | 0.00017666 |
| **pL7** | 231.282 | **pR7** | 231.187 | 0.00011415 |
| **pL8** | 231.123 | **pR8** | 231.259 | 0.00016344 |
| **pL9** | 231.183 | **pR9** | 231.14 | 5.1684E-05 |
| **pL10** | 231.24 | **pR10** | 231.151 | 0.00010697 |
| **pL11** | 231.245 | **pR11** | 231.197 | 5.7687E-05 |
| **pL12** | 231.172 | **pR12** | 231.126 | 5.5294E-05 |
| **pL13** | 231.183 | **pR13** | 231.204 | 2.5242E-05 |
| **pL14** | 231.121 | **pR14** | 231.235 | 0.000137 |
| **pL15** | 231.099 | **pR15** | 231.225 | 0.00015143 |
| **pL16** | 231.031 | **pR16** | 231.202 | 0.00020554 |
| **pL17** | 230.98 | **pR17** | 231.257 | 0.00033287 |
| **pL18** | 230.967 | **pR18** | 231.266 | 0.00035931 |

$$\varepsilon_x = \frac{zR - zL}{l} \tag{14}$$

To find the translational error along the Z-axis, other measurements were done. The measurements were also done in the same 18 points, but the measurements were done on the laser's tip.

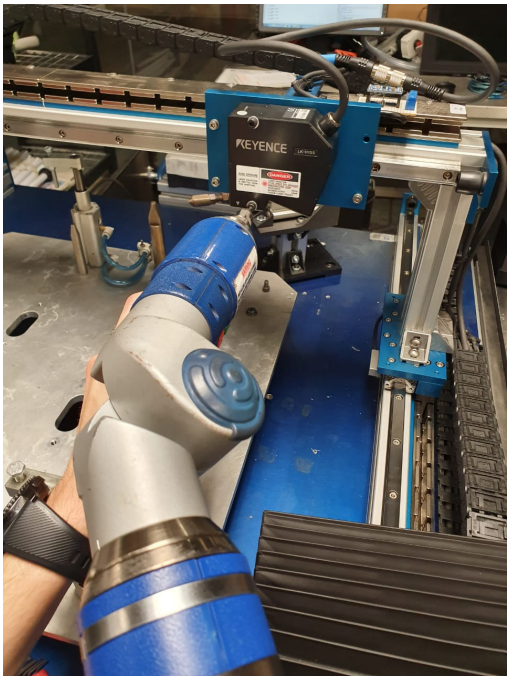


Figure 30. Measured point on the laser

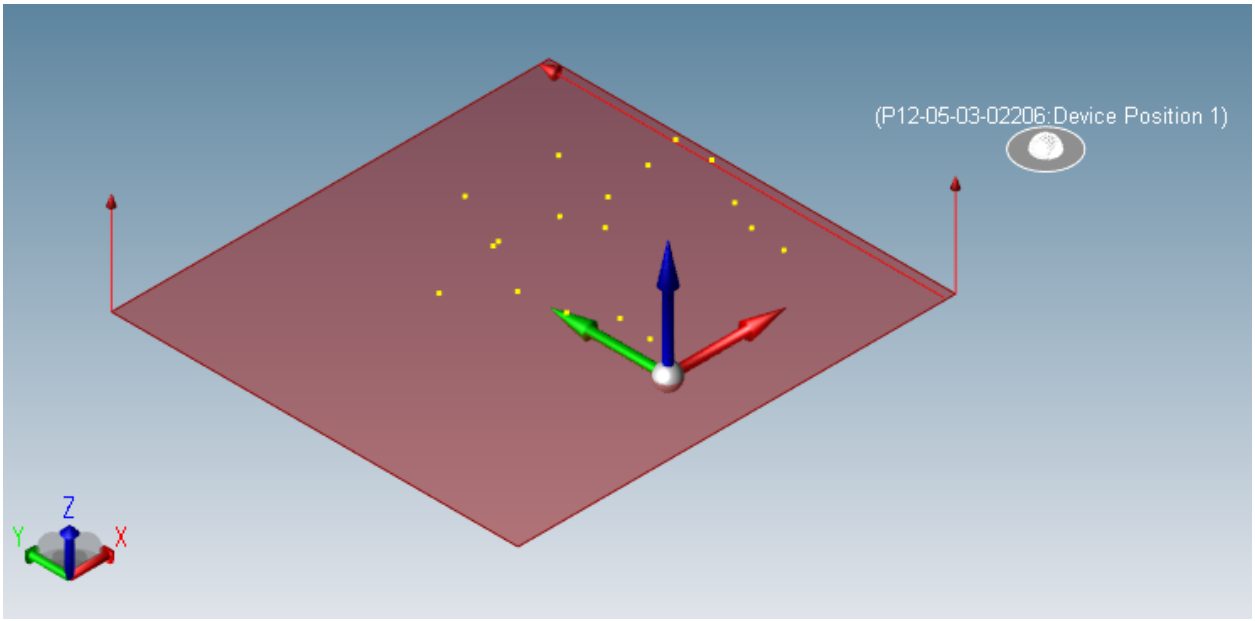


Figure 31. Points generated by the FaroArm.

Table 9. Translational Z-axis error in each measuring point.

| Feature | dz |
|---|---|
| p1 | 0 |
| p2 | 0.001 |
| p3 | 0.006 |
| p4 | 0.01 |
| p5 | 0.04 |
| p6 | -0.056 |
| p7 | -0.053 |
| p8 | -0.051 |
| p9 | -0.038 |
| p10 | 0.034 |
| p11 | 0.006 |
| p12 | -0.014 |
| p13 | -0.003 |
| p14 | 0.015 |
| p15 | -0.047 |
| p16 | 0.02 |
| p17 | -0.038 |
| p18 | -0.048 |

The previous analysis was done to obtain the first HTM, [T1], for the second one [T2], we will analyze angular errors respecting another plane:

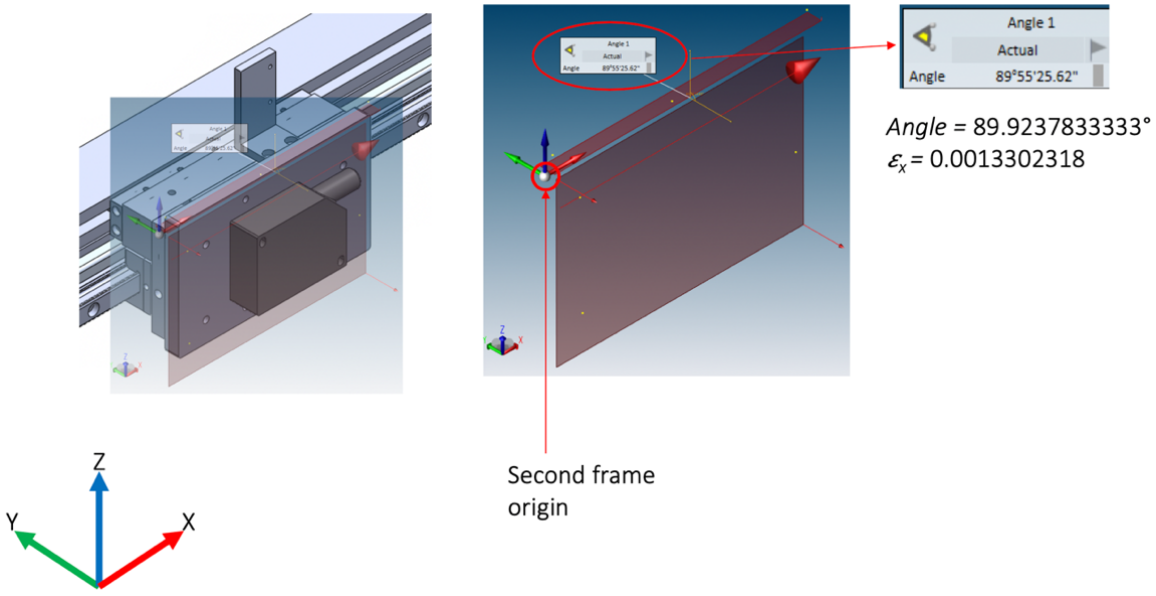


Figure 32. Second frame analysis using FaroArm.

The error angle of the second frame is:

$\varepsilon_x$ = 0.0013302318

### 5.2 Total errors with HTM analysis

The transformation matrices were done with two frames, besides the origin.

**First frame:**

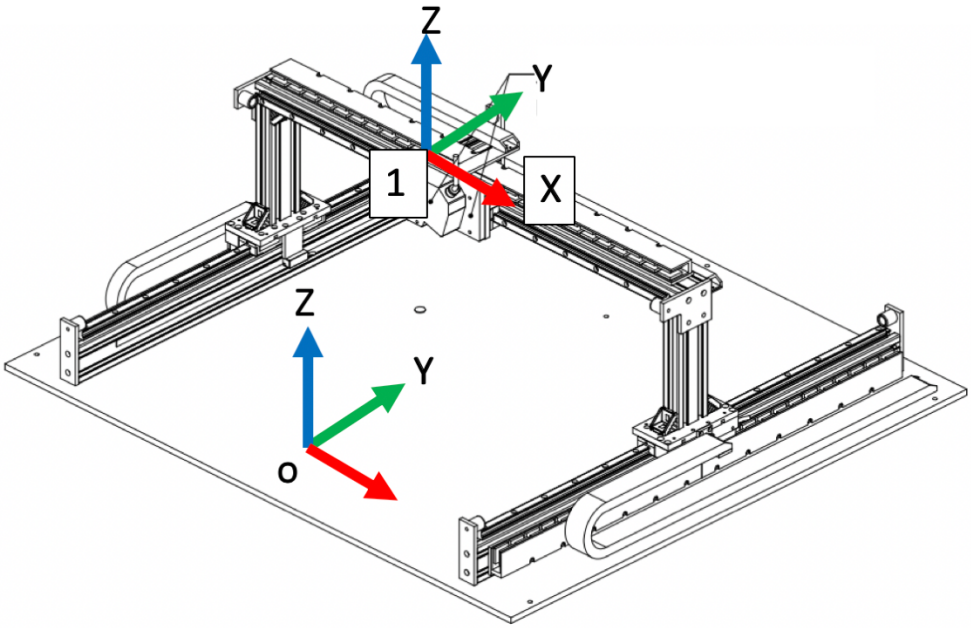


Figure 33. Origin and Frame 1

The first transformation matrix, equation 15, is obtained by substituting the variable error values found across Section 4.2 and the positions given by the encoders.

$$T_1 = \begin{bmatrix} 1 & -\varepsilon_z & \varepsilon_y & X + \delta_x \\ \varepsilon_z & 1 & -\varepsilon_x & Y + \delta_y \\ -\varepsilon_y & \varepsilon_x & 1 & 357.056 + \delta_z \\ 0 & 0 & 0 & 1 \end{bmatrix} \quad (15)$$

Where the angular and translational errors are changing variables depending on the Point measured.

Table 10. Error parameters values in each point

| Position | Linear Errors | | | Rotational errors (Roll, Pitch, Yaw) | | |
|---|---|---|---|---|---|---|
| | $\delta_x$ | $\delta_y$ | $\delta_z$ | $\varepsilon_x$ | $\varepsilon_y$ | $\varepsilon_z$ |
| 1 | 1E-3 | 28 | 0 | 0.03 | 0.00027155 | 6.74699E-05 |
| 2 | 1E-3 | 30 | 0.001 | 0.02 | 0.00021989 | 7.22892E-05 |
| 3 | 1E-3 | 20 | 0.006 | 0.03 | 9.7327E-05 | 4.81928E-05 |
| 4 | 1E-3 | 25 | 0.01 | 0.02 | 9.3742E-05 | 6.0241E-05 |
| 5 | 1E-3 | 25.5 | 0.04 | 0.04 | 0.00033899 | 6.14458E-05 |
| 6 | 1E-3 | 26 | -0.056 | 0.02 | 0.00017666 | 6.26506E-05 |
| 7 | 1E-3 | 32 | -0.053 | 0.01 | 0.00011415 | 7.71084E-05 |
| 8 | 1E-3 | 16 | -0.051 | 0.03 | 0.00016344 | 3.85542E-05 |
| 9 | 1E-3 | 32.5 | -0.038 | 0.03 | 5.1684E-05 | 7.83133E-05 |
| 10 | 1E-3 | 35.5 | 0.034 | 0.01 | 0.00010697 | 8.55422E-05 |
| 11 | 1E-3 | 46 | 0.006 | 0.01 | 5.7687E-05 | 0.000110843 |
| 12 | 1E-3 | 16.5 | -0.014 | 0.01 | 5.5294E-05 | 3.9759E-05 |
| 13 | 1E-3 | 31.5 | -0.003 | 0.01 | 2.5242E-05 | 7.59036E-05 |
| 14 | 1E-3 | 26 | 0.015 | 0.01 | 0.000137 | 6.26506E-05 |
| 15 | 1E-3 | 28 | -0.047 | 0.01 | 0.00015143 | 6.74699E-05 |
| 16 | 1E-3 | 26.5 | 0.02 | 0.02 | 0.00020554 | 6.38554E-05 |
| 17 | 1E-3 | 17.5 | -0.038 | 0.01 | 0.00033287 | 4.21687E-05 |
| 18 | 1E-3 | 17 | -0.048 | 0.03 | 0.00035931 | 4.09639E-05 |

**Second Frame:**

The second frame is located at the top of the plate holding the laser.

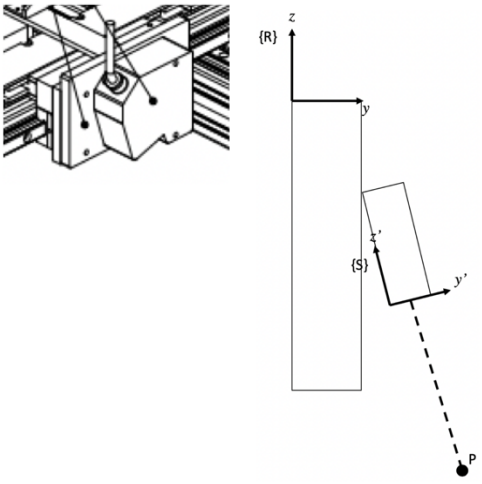


Figure 34. Second frame diagram

$$T_2 = \begin{bmatrix} 1 & 0 & 0 & -38.64 \\ 0 & 1 & -\varepsilon_x & -19.798 \\ 0 & \varepsilon_x & 1 & -83.283 \\ 0 & 0 & 0 & 1 \end{bmatrix} \quad (16)$$

Where $\varepsilon_x = 0.0013302318$

Applying equations 9 to 11, The errors in each axis are found and can be seen in Table 11:

Table 11. Error parameters

| Measure point | Error in X | Error in Y | Error in Z |
|---|---|---|---|
| **1** | 61.0204622 | -212.75831 | -3.619044 |
| **2** | 48.8728479 | -173.85652 | -6.059598 |
| **3** | 20.755663 | -205.50317 | -2.8868783 |
| **4** | -24.054605 | -169.32207 | -2.9409083 |
| **5** | -81.290118 | -251.20664 | -16.590764 |
| **6** | -43.445142 | -170.22896 | 66.2629978 |
| **7** | -29.147816 | -134.95474 | 57.4107787 |
| **8** | 36.3684533 | -201.87561 | 51.558524 |
| **9** | -14.59909 | -216.83932 | 46.8708877 |
| **10** | -27.639684 | -138.12886 | -29.86653 |
| **11** | -16.640108 | -147.65123 | -3.7709782 |
| **12** | -14.682176 | -120.89792 | 16.1365747 |
| **13** | 3.39375801 | -134.5013 | 2.02466113 |
| **14** | 29.7262735 | -129.51339 | -20.293717 |
| **15** | 32.9511029 | -132.23407 | 41.1485576 |
| **16** | 45.6916493 | -170.6824 | -24.505169 |
| **17** | 75.8218425 | -121.80482 | 25.1380161 |
| **18** | 82.0143032 | -202.7825 | 40.9900808 |
| **Max error** | **82.0143032** | **-251.20664** | **66.2629978** |


Figure 35. Error values

The error found In the Z-axis was from 2.02 to 66.26 μm. The R&R test the range was from 13 to 44 μm. Although angular errors are presented, the major problem is the error caused by $\delta_z$ on different points. The HTM model is useful to find additional factors to the variance in the Z-axis besides thermal, Hertz or angular errors.

This analysis contributes for the continuous improvement of the digital twin.

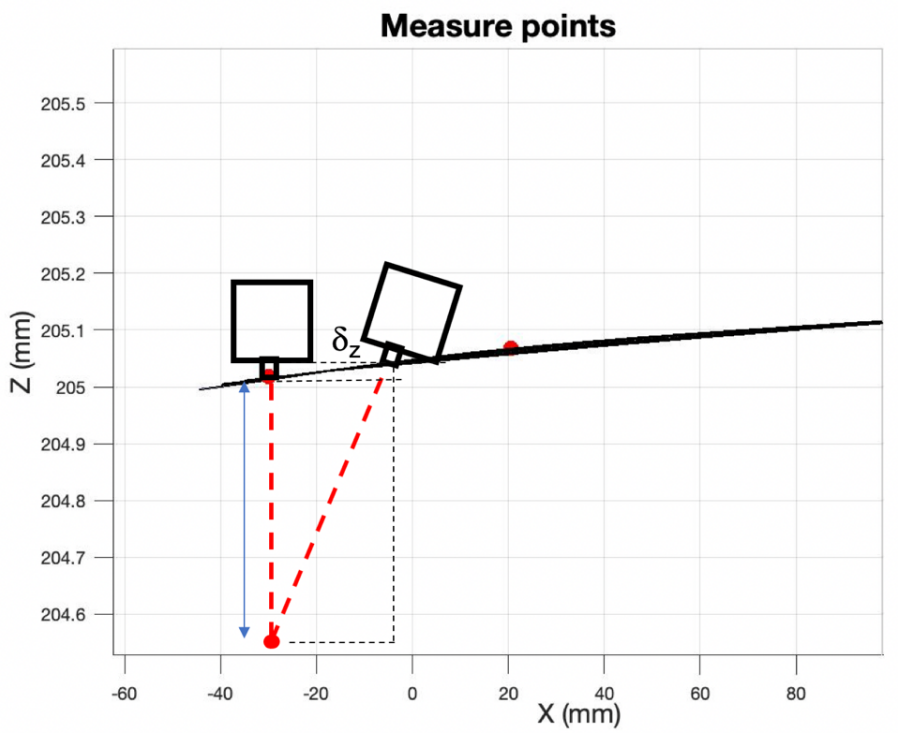


Figure 36. Laser displacement

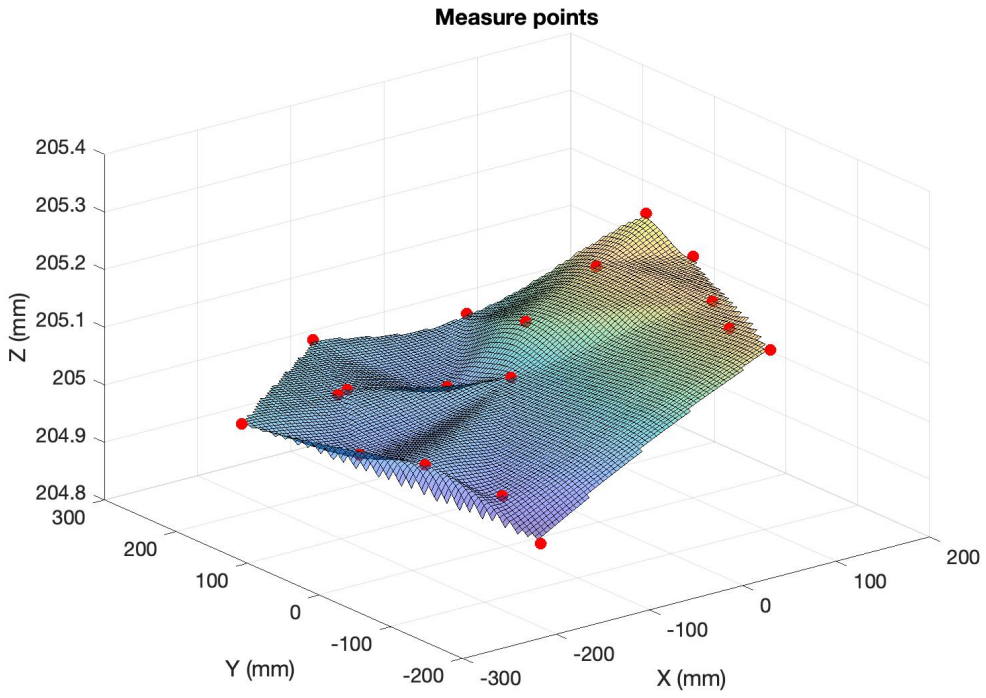


Figure 37. Surface generated by measuring points (isometric view)

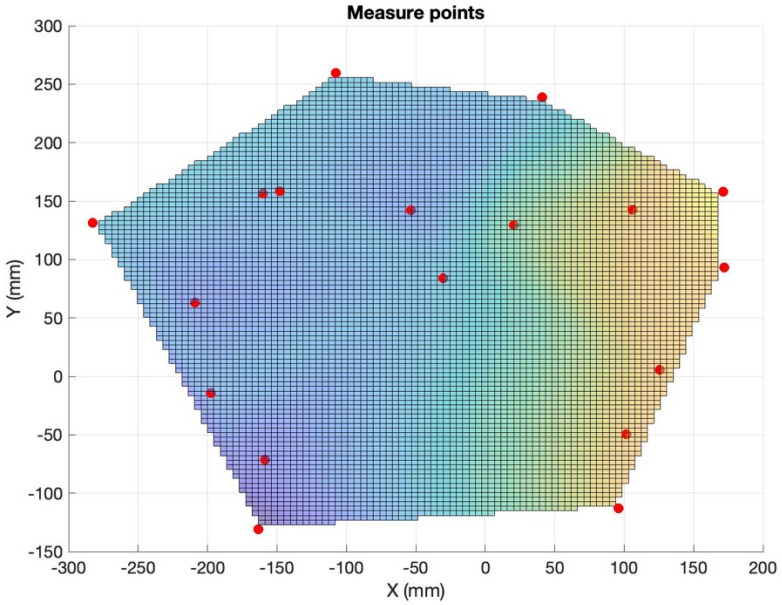


Figure 38. Surface generated by measuring points (top view)

A surface that goes through all the points is generated to find the slope between points. This is done to find the position and angle that the laser might have at the desired position. The error is calculated by using the slope and the Y and Z axes position errors:

Table 12. Errors caused by the slope

| Points | Slope | Error |
|---|---|---|
| 2 | 1.5699E-05 | -0.0027293 |
| 3 | 0.00010902 | -0.0224035 |
| 4 | 0.00011399 | -0.0193017 |
| 5 | 0.00062043 | -0.1558571 |
| 6 | 0.00365344 | -0.6219221 |
| 7 | 0.00401941 | -0.5424391 |
| 8 | 0.00112127 | -0.2263578 |
| 9 | -0.0006503 | 0.14100957 |
| 10 | 0.00035276 | -0.0487262 |
| 11 | 0.00028795 | -0.0425161 |
| 12 | 0.00013893 | -0.016796 |
| 13 | 0.00130321 | -0.1752841 |
| 14 | -0.0005953 | 0.07709437 |
| 15 | 0.00069011 | -0.0912562 |

| | | |
|---|---|---|
| 16 | -0.0002581 | 0.04405617 |
| 17 | 0.00066437 | -0.0809235 |
| 18 | 0.0008092 | -0.1640912 |

The laser's resolution is 0.25 micrometers, according to results in Table 12, all points except for 6 and 7, have smaller errors than the laser's sensor.

# Chapter 6: Conclusions and future work

## 6.1 Conclusions

The general HTM analysis is able to characterize various multi-axis machine tools. This thesis described how the HTM is implemented and it was used to calculate the error parameters presented in the laser measurement's gantry system. At the beginning, prior work quantified the errors caused by Hertz stresses and temperature, but they were not the only causes of deviations in the Z axis measures.

New data was obtained from sensors already mounted in the system and from a new implemented IMU, which is used to obtain angular errors in the X-axis. This was done for monitoring the system and set new normal condition parameters on the machine. The IMU presented angles from 0.01 to 0.04 degrees in each measuring position. The errors caused the angular deflections were even smaller than the deviation caused by the laser sensor.

The HTM model is able to estimate errors depending on the position reached by the system and can be easily manipulated to add more measurement points or change coordinates. This is true about obtaining data from the encoders and the IMU, mpu 6050

sensor, but not for finding the error caused by the difference in height between measuring points. As explained in previous chapters, some errors were measured by the FaroArm, therefore in order to add or change measuring position points, a new experiment needs to be done.

The IMU, mpu 6050 was able to start taking measures once the machine cycle started for correct synchronization with the encoder's sensors. This helped to obtain the angular orientation of the system on each one of the 18 tested positions. This was important to determine if the IMU sensor could give reliable information for the experiments. The implementation of this sensor in the system is useful to continue developing the digital twin by setting new normal operation parameters in the machine.

The established objectives were fulfilled the use of the sensors discusses on the thesis. HTM matrices were done by the recollected data of the errors. The encoders were able to provide accurate position of each individual motor. The IMU sensor was able to give reliable data and showed errors within the prior known data in the R&R tests.

### 6.2 Future Work

In present work, data analysis is done by using computing tools, Matlab, the development of an automatic analysis tool could generate more valuable data for predictive measures. It can also save time for further analysis to continue developing new functions on the machine.

A feature to implement a web app that notifies the user when the error gets out of range and take corrective actions.

A real time simulation can be done by continuing to work for a Dynamic model of the PMLSMs. This can simulate mechanical errors in position to warn the system when the machine range surpass acceptable tolerances and run real-time scenarios.

The dynamic model on the motors can also provide information about the performance of the motors and could be useful for developing a full cyberphysical system of the machine.

# Appendix A:

MPU 6050 specifications

| |
|---|
| Digital output of 6 axes |
| Sensibility of ± 250, ± 500, ± 1000, and ± 2000dps |
| Embedded algorithms for calibration |
| Programmable interruptions |

FaroArm measured points coordinates

| Point | x | y | z | Point | x | y | z | $\varepsilon y$ |
|---|---|---|---|---|---|---|---|---|
| **pL0** | -421.214 | 39.372 | 231.284 | **pR0** | 411.02 | 33.646 | 231.418 | 0.00016101 |
| **pL1** | -420.718 | 15.303 | 231.069 | **pR1** | 411.527 | 9.649 | 231.295 | 0.00027155 |
| **pL2** | -420.194 | 71.327 | 231.091 | **pR2** | 412.044 | 65.676 | 231.274 | 0.00021989 |
| **pL3** | -419.635 | 135.713 | 231.124 | **pR3** | 412.613 | 130.094 | 231.205 | 9.7327E-05 |
| **pL4** | -418.75 | 215.165 | 231.307 | **pR4** | 413.324 | 209.317 | 231.229 | 9.3742E-05 |
| **pL5** | -418.078 | 279.192 | 231.394 | **pR5** | 413.81 | 273.873 | 231.112 | 0.00033899 |
| **pL6** | -418.145 | 273.17 | 231.399 | **pR6** | 413.969 | 267.823 | 231.252 | 0.00017666 |
| **pL7** | -418.401 | 262.001 | 231.282 | **pR7** | 413.833 | 256.798 | 231.187 | 0.00011415 |
| **pL8** | -416.783 | 229.41 | 231.123 | **pR8** | 415.329 | 218.349 | 231.259 | 0.00016344 |
| **pL9** | -415.843 | 288.45 | 231.183 | **pR9** | 416.14 | 277.274 | 231.14 | 5.1684E-05 |
| **pL10** | -414.383 | 382.446 | 231.24 | **pR10** | 417.596 | 371.268 | 231.151 | 0.00010697 |
| **pL11** | -414.242 | 395.462 | 231.245 | **pR11** | 417.836 | 384.291 | 231.197 | 5.7687E-05 |
| **pL12** | -415.53 | 307.415 | 231.172 | **pR12** | 416.381 | 296.211 | 231.126 | 5.5294E-05 |
| **pL13** | -415.537 | 305.422 | 231.183 | **pR13** | 416.42 | 294.355 | 231.204 | 2.5242E-05 |
| **pL14** | -415.954 | 283.311 | 231.121 | **pR14** | 416.157 | 272.341 | 231.235 | 0.000137 |
| **pL15** | -417.06 | 213.278 | 231.099 | **pR15** | 414.981 | 202.323 | 231.225 | 0.00015143 |
| **pL16** | -418.219 | 138.297 | 231.031 | **pR16** | 413.734 | 127.236 | 231.202 | 0.00020554 |
| **pL17** | -419.134 | 78.248 | 230.98 | **pR17** | 413.03 | 67.684 | 231.257 | 0.00033287 |
| **pL18** | -420.032 | 19.254 | 230.967 | **pR18** | 412.118 | 8.685 | 231.266 | 0.00035931 |

## Bibliography:


[1] J. Ni and X. Huang, “Discovery-to-Recall in the Automotive Industry: A Problem-Solving Perspective on Investigation of Quality Failures,” *J. Supply Chain Manag.*, 2018.

[2] T. Eifler and T. J. Howard, “The importance of robust design methodology: case study of the infamous GM ignition switch recall,” *Res. Eng. Des.*, 2018.

[3] R. W. Bagshaw and S. T. Newman, “Manufacturing data analysis of machine tool errors within a contemporary small manufacturing enterprise,” *Int. J. Mach. Tools Manuf.*, vol. 42, no. 9, pp. 1065–1080, 2002.

[4] A. G. Frank, L. S. Dalenogare, and N. F. Ayala, “Industry 4.0 technologies: Implementation patterns in manufacturing companies,” *Int. J. Prod. Econ.*, 2019.

[5] W. Kritzinger, M. Karner, G. Traar, J. Henjes, and W. Sihn, “Digital Twin in manufacturing: A categorical literature review and classification,” *IFAC-PapersOnLine*, vol. 51, no. 11, pp. 1016–1022, 2018.

[6] E. Negri, L. Fumagalli, and M. Macchi, “A Review of the Roles of Digital Twin in CPS-based Production Systems,” *Procedia Manuf.*, vol. 11, no. June, pp. 939–948, 2017.

[7] D. Guamán, “Mechatronic Design of a Fast-Non-Contact Measurement System for Inspection of Castings Parts in Production Line,” 2018.

[8] A. P. Castro, “Design of the technological infrastructure for data acquisition of an in-line measuring Industry 4 . 0 compatible machine,” 2017.

[9] H. W. Ko *et al.*, “Quasistatic error modeling and model testing for a 5-axis machine with a redundant axis,” *J. Manuf. Process.*, 2018.

[10] C. Li, B. Yao, and Q. Wang, “Modeling and Synchronization Control of a Dual Drive Industrial Gantry Stage,” *IEEE/ASME Trans. Mechatronics*, vol. 23, no. 6, pp. 2940–2951, 2018.

[11] F. J. Lin, P. H. Chou, C. S. Chen, and Y. S. Lin, “Three-degree-of-freedom dynamic model-based intelligent nonsingular terminal sliding mode control for a gantry position stage,” *IEEE Trans. Fuzzy Syst.*, vol. 20, no. 5, pp. 971–985, 2012.

[12] W. Fan, H. Lu, X. Zhang, Y. Zhang, R. Zeng, and Q. Liu, “Two-degree-of-freedom dynamic model-based terminal sliding mode control with observer for dual-driving feed stage,” *Symmetry (Basel).*, vol. 10, no. 10, 2018.

[13] A. H. Slocum, “Precision machine design: Macromachine design philosophy and its applicability to the design of micromachines,” 1992.

[14] Y. Echerfaoui, A. El Ouafi, and A. Chebak, “Laser Interferometer Based Measurement for Positioning Error Compensation in Cartesian Multi-Axis Systems,” *J. Anal. Sci. Methods Instrum.*, 2017.

[15] J. Yin, M. Li, and F. Pan, “Modeling quasi-static errors in a five-axis gantry machine tool,” *Appl. Mech. Mater.*, vol. 152–154, pp. 781–787, 2012.

[16] B. Zhou, S. Wang, C. Fang, S. Sun, and H. Dai, “Geometric error modeling and compensation for five-axis CNC gear profile grinding machine tools,” *Int. J. Adv. Manuf. Technol.*, 2017.

[17] Y. Hsu and H. Lee, “A Simplified Approach to Measure 21 Forms of Geometric Error for Three-axis Machine Tools : Principles and Application,” *Sci. Coop. Int. J. Mech. Aerosp. Eng.*, vol. 1, no. 1, pp. 39–46, 2015.

[18] Y. Lin and Y. Shen, “A generic kinematic error model for machine tools.”
[19] G. Fu, J. Fu, H. Gao, and X. Yao, “Squareness error modeling for multi-axis machine tools via synthesizing the motion of the axes,” *Int. J. Adv. Manuf. Technol.*, 2017.
[20] Rajeevlochana C.G., S. K. Saha, and S. Kumar, “Automatic Extraction of DH Parameters of Serial Manipulators using Line Geometry,” 2012.
[21] J. Faiz, M. Manoochehri, and G. Shahgholian, “A novel robust design for LPMSM with minimum motor current THD based on improved space vector modulation technique,” *Jt. Int. Conf. - ACEMP 2015 Aegean Conf. Electr. Mach. Power Electron. OPTIM 2015 Optim. Electr. Electron. Equip. ELECTROMOTION 2015 Int. Symp. Adv. Electromechanical Moti*, pp. 1–7, 2016.
[22] K. Alicemary, B. Arundhati, and M. P. Maridi, “Modelling, Simulation and Nonlinear Control of Permanent Magnet Linear Synchronous Motor,” *Int. J. Adv. Res. Electr. Electron. Instrum. Eng.*, vol. 1, no. 6, pp. 555–562, 2013.
[23] H. Technologies, “Single Rail Positioning Stage H-Gantry.”
[24] W. Qin and F. Machining, “Modeling and compensation of errors,” 2013.